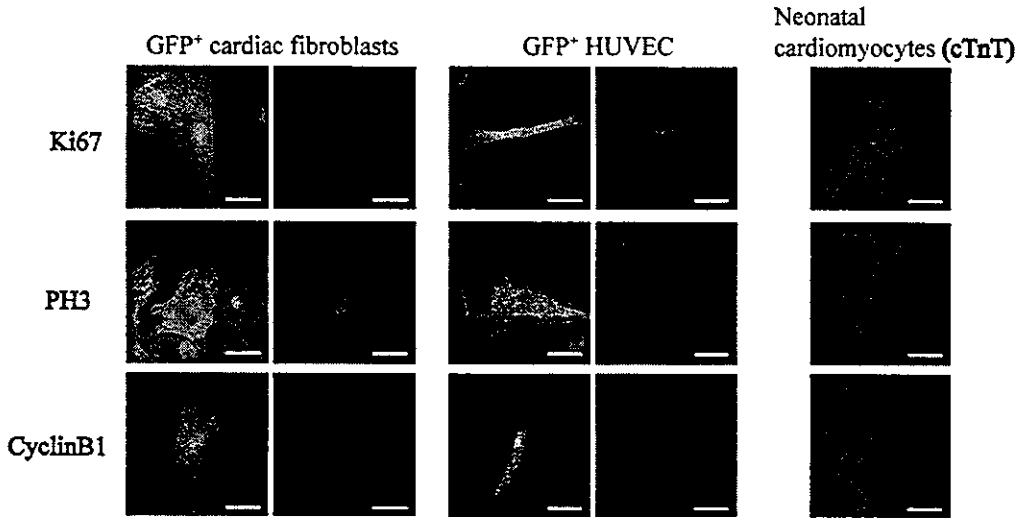

Figure 4. **Localization of Ki67, PH3, and cyclinB1 in cFB, HUVEC, and neonatal cardiomyocytes.** GFP+ cFB, GFP+ HUVEC, and neonatal rat cardiomyocytes were stained with mouse monoclonal anti-Ki67 (top row, red), rabbit polyclonal anti-PH3 (middle row, red), and mouse monoclonal anti-cyclinB1 (bottom row, red). Cardiomyocytes were identified with anti-cTnT antibodies (blue). HUVEC and cFB expressed Ki67, PH3, and cyclinB1. Some of neonatal cardiomyocytes expressed Ki67, but not PH3 or cyclinB1. Bars, 50 μm.

nocodazole. These results suggest that some cardiomyocytes reenter the stage of mitosis after fusion with HUVEC and cFB. Mitosis of fused cardiomyocytes was confirmed by the existence of cells that showed visible chromosomes characteristic of the several distinct phases of mitosis (Fig. 6 C). In Fig. 6, GFP+ cardiomyocytes fused with RFP+ HUVEC (b and j) or RFP+ cFB (f) show prophase chromosomes (c), metaphase chromosomes (g), and anaphase chromosomes (k).

Cardiomyocytes spontaneously fuse with surrounding somatic cells in vivo

Next, we examined whether cardiomyocytes fuse with other mature somatic cells in vivo as well as in vitro. RFP+ HUVEC or RFP+ skeletal muscle–derived cells isolated from neonatal Sprague-Dawley rats were first injected into the hearts of adult GFP transgenic Sprague-Dawley rats. At 7 d after injection, we observed GFP and RFP double-positive cells, which also expressed cTnT, in the heart (Fig. 7 A). The expression of two different kinds of dyes in the single cell suggests that spontaneous cell fusion could also occur in vivo in the heart. Furthermore, we examined the cell fusion in vivo by using the Cre/lox recombination assay. HUVEC infected with adenovirus containing the nuclear-localized Cre recombinase gene (Kanegae et al., 1995) were transplanted directly to the heart of mice that carry the loxP-flanked chloramphenicol acetyltransferase (CAT) gene located between the CAG promoter and the *LacZ*

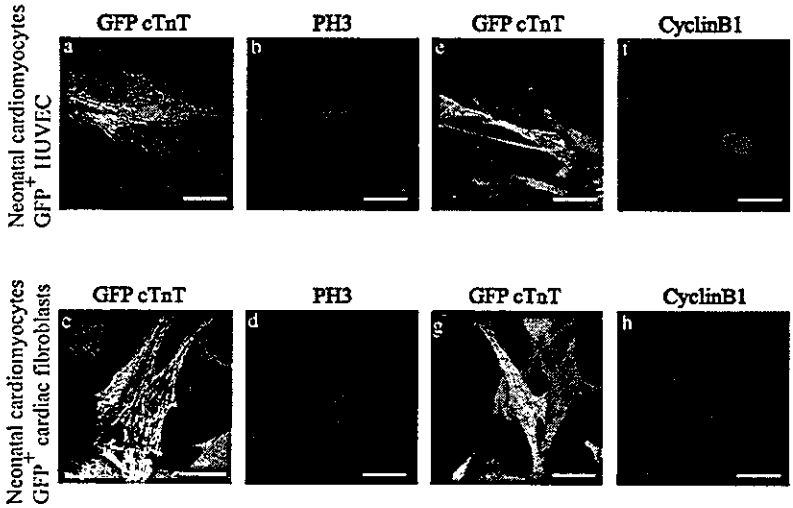

Figure 5. **Neonatal rat cardiomyocytes expressed PH3 and cyclinB1 after cell fusion with HUVEC or cFB.** Neonatal rat cardiomyocytes were cocultured with GFP+ HUVEC or GFP+ cFB and double stained with anti-cTnT (red) and anti-PH3 (blue) or anti-cyclinB1 (blue) antibodies. Fused cells between cardiomyocytes and HUVEC or cFB coexpressed both GFP and cTnT (a, c, e, and g, yellow in merged images), and expressed PH3 (b and d, blue) and cyclinB1 (f and h, blue) in their nuclei. Bars, 50 μm.

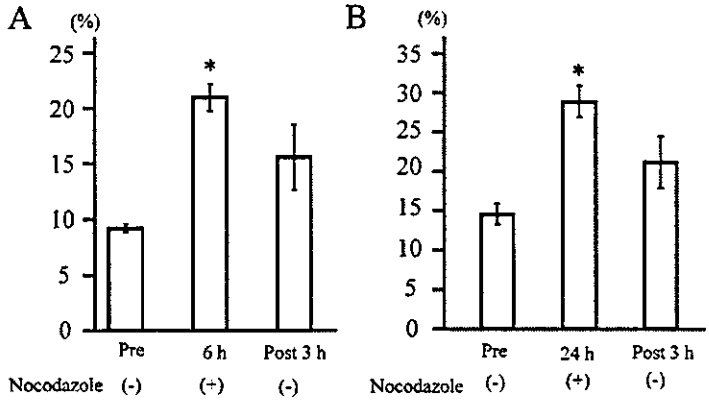

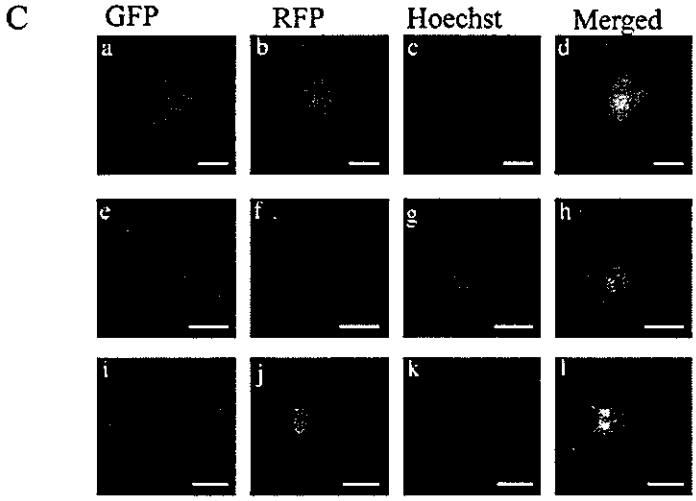

Figure 6. **Cardiomyocytes of neonatal rats reentered the cell cycle through cell fusion with HUVEC or cFB in vitro.** (A and B) Quantitative analysis of the percentage of PH3-expressing cardiomyocytes fused with HUVEC or cFB. The percentage of PH3-expressing cardiomyocytes in all fused cells with HUVEC (A) and cFB (B) was significantly increased with the treatment with nocodazole, and was decreased after the withdrawal of nocodazole. Data are mean ± SD of four independent experiments. *, $P < 0.05$ vs. pretreatment. (C) Fluorescent images of GFP^+ cardiomyocytes fused with RFP^+ HUVEC (top and bottom rows, a–d and i–l) or RFP^+ cFB (middle row, e–h) stained with Hoechst 33258 (blue). Typical prophase chromosome (c), metaphase chromosome (g), and anaphase chromosome (k) were visualized by Hoechst staining. Merged fluorescent images indicate that fused cells show mitotic figures. Bars, 50 μm.

gene (Fig. 8 A, CAG-CAT-*LacZ*). At 4 d after transplantation, some β-gal$^+$ cells were observed in the myocardium, and the same cells in the adjacent sections showed the expression of Cre and cTnT with the fine striated pattern. A typical image was presented in Fig. 8 B. Skeletal muscle–derived cells isolated from CAG-CAT-*LacZ* mice were transplanted to the heart of MerCreMer mice (Sohal et al., 2001) in which the expression of Cre was restricted to the cardiomyocytes under the control of the αMHC promoter after treatment with tamoxifen (Fig. 8 C). At 4 d after transplantation, we observed some β-gal$^+$ cells that coexpressed Cre and cTnT in the myocardium (Fig. 8 D). These genetic results strongly suggest that HUVEC and skeletal muscle–derived cells could fuse spontaneously with cardiomyocytes in vivo. Next, we examined whether cardiomyocytes spontaneously fuse with endogenous surrounding cells in injured heart tissue. When adult rat hearts were cryoinjured there were cells expressing both cTnT and vWF at the border zone, but not at the normal and injured areas (Fig. 7 B). Staining of adjacent sections revealed that cells that expressed both cTnT and vWF also expressed desmin and Ki67 (Fig. 7 B), whereas there were no Ki67-expressing cardiomyocytes in the normal adult heart. These findings suggest that cardiomyocytes fuse with surrounding endothelial lineage cells and reenter the cell cycle also in vivo.

Bone marrow-derived cells and EPCs can fuse with cardiomyocytes in vitro

Our in vitro and in vivo results suggest that cells expressing both cTnT and vWF in the damaged heart are fusion products of cardiomyocytes and endothelial cells. However, it has been reported that bone marrow–derived cells and EPCs differentiate into vascular cells and cardiomyocytes (Jackson et al., 2001; Badorff et al., 2003), leading us to examine whether bone marrow–derived or peripheral blood–derived EPCs may fuse with cardiomyocytes and express cTnT and vWF. Hematopoietic cells and mesenchymal cells from bone marrow of GFP transgenic mouse and human-derived EPCs were cocultured with neonatal cardiomyocytes that were infected with the adenoviral vector carrying the *LacZ* reporter gene. When GFP^+ bone marrow–derived mesenchymal cells were cocultured with $LacZ^+$ neonatal rat cardiomyocytes, ~0.01% of GFP^+ cells expressed cTnT and β-gal, suggesting that bone marrow–derived mesenchymal cells express cardiac-specific protein through cell fusion with cardiomyocytes (Fig. 9 A, a–d, arrow). In con-

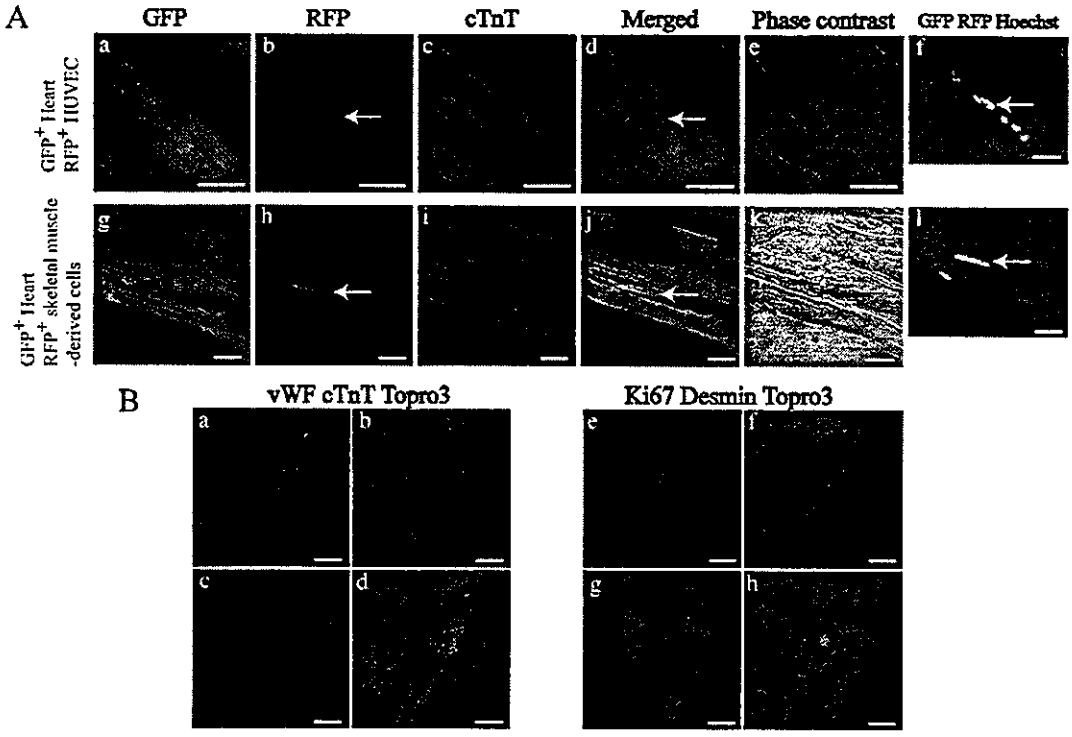

Figure 7. **Adult cardiomyocytes fused with somatic cells in vivo.** (A) RFP+ HUVEC or RFP+ skeletal muscle–derived cells were injected to the heart of GFP transgenic rats, and 6-μm sections were stained with rabbit polyclonal anti-RFP and mouse monoclonal anti-cTnT antibodies. Confocal microscopic images demonstrate that GFP+ cardiomyocytes (a and g, green) coexpress RFP, marker proteins of HUVEC (b, red) and skeletal muscle–derived cells (h, red), and cTnT (c and i, blue). d and j represent merged images; e and k represent phase-contrast images. The merged images of the same view were taken by fluorescent microscope (f and l). Nuclei were stained with Hoechst 33258 (f and l, blue). Arrows indicate the fused cells. Bars, 100 μm. (B) Two adjacent sections of 6 μm were cut from cryoinjured adult rat hearts. One section (a–d) was triple stained with mouse monoclonal anti-cTnT (red), rabbit polyclonal anti-vWF (green) antibodies, and Topro3 (blue). Another section (e–h) was triple stained with rabbit polyclonal anti-desmin (red), mouse monoclonal anti-Ki67 (green) antibodies, and Topro3 (blue). Confocal microscopic images in the border zone of cryoinjured hearts show a cell expressing vWF (a) and cTnT (b) with nucleus stained by Topro3 (c). Right panel shows a same fine-striated cell that expresses desmin (f) and Ki67 (e) with nucleus stained by Topro3 (g). d and h represent merged images. Bars, 100 μm.

trast, GFP+ hematopoietic cells expressed neither cTnT nor β-gal when cocultured with *LacZ*+ neonatal rat cardiomyocytes. Next, we isolated human-derived EPCs from the healthy volunteers and cultured them as described previously (Kalka et al., 2000). At 7 d after starting culture, spindle-shaped cells were stained with DiI-AcLDL and FITC-labeled ulex europaeus agglutinin-1 (UEA-1) lectin (Fig. 9 B, a and b), suggesting that these adherent cells were endothelial lineage cells. Immunocytochemical analysis revealed that ~30% of these cells expressed vWF at this time (Fig. 9 B, c). When human-derived EPCs were cocultured with neonatal mouse cardiomyocytes that were infected with the adenoviral vector carrying the *LacZ* reporter gene, ~0.1% of vWF-expressing cells expressed cTnT and β-gal (Fig. 9 C, a–d). Hoechst nuclear staining (Blau et al., 1983) revealed that these cells contained both a human-derived nucleus (smoothly appearance) and a mouse-derived nucleus (punctate appearance) (Fig. 9 C, e–h), suggesting that human-derived EPCs express cardiac-specific proteins through cell fusion with cardiomyocytes. These results suggest that bone marrow–derived mesenchymal cells and circulating EPCs, but not hematopoietic cells, fuse with cardiomyocytes.

Discussion

In this paper, we show that cardiomyocytes fuse with various types of cells including endothelial cells, cFB, bone marrow–derived mesenchymal cells, and EPCs in vitro. In the cells generated by fusion between cardiomyocytes and HUVEC or cFB, the cardiac phenotype became dominant until at least 7 d after starting coculture, and some fused cells reentered the cell cycle maintaining the cardiac phenotype. Moreover, cardiomyocytes fused with transplanted cells and surrounding cells in vivo as well as in vitro.

Heterokaryons have been used to determine whether specific traits of either parental cells are maintained or extinguished (Baron, 1993; Blau and Blakely, 1999). In this work, we identified fused cells retrovirally induced by two different fluorescent dyes. Analysis of lineage-specific marker proteins revealed that the phenotype of cardiomyocytes became more dominant than that of HUVEC and cFB as time passed. Besides the contractile proteins, a cardiac-specific secreted protein (ANF) and a cardiac-selective transcription factor (GATA4) were also expressed in the fused cells over 7 d. Moreover,

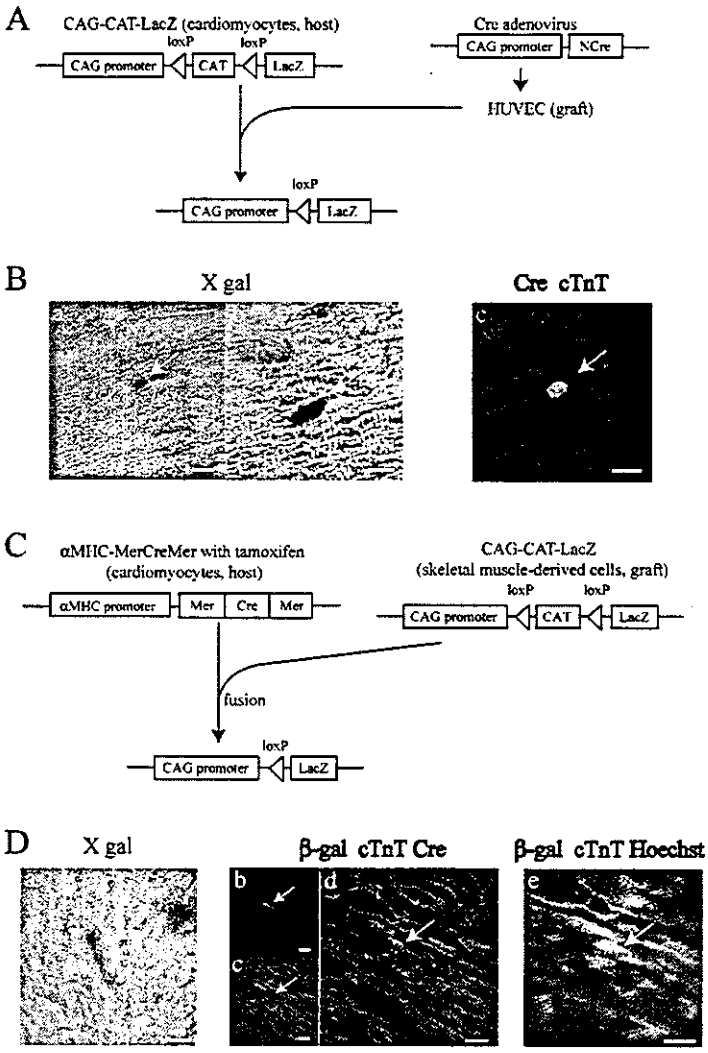

Figure 8. **Cre/lox recombination assay for detection of cell fusion in vivo.** (A and C) Schematic representation of the transgenes expressed by the mouse line and the adenovirus used in HUVEC transplantation model (A) and in skeletal muscle–derived cell transplantation model (C). (B) Cre-expressing HUVEC were transplanted to the heart of CAG-CAT-*LacZ* mice. Two adjacent sections of 6 μm were prepared. One section treated with X-gal staining demonstrated a β-gal$^+$ cell in the myocardium (a and b, arrow). The adjacent section, which was double stained with mouse monoclonal anti-Cre and goat polyclonal anti-cTnT antibodies, showed the expression of Cre (c, green, arrow) and cTnT (c, red, arrow) with the fine-striated pattern in the same cell in a and b. Bars: a, 50 μm; b and c, 100 μm. (D) Skeletal muscle–derived cells isolated from CAG-CAT-*LacZ* mice were transplanted to the heart of MerCreMer mice treated with tamoxifen. Sections were analyzed by X-gal staining or by triple staining with rabbit polyclonal anti-β-gal, goat polyclonal anti-cTnT, and mouse monoclonal anti-Cre antibodies. X-gal staining revealed a β-gal$^+$ cell in the myocardium (a). The immunofluorescent confocal images demonstrated that β-gal$^+$ (b and d, green) cells also expressed cTnT (c and d, red) and Cre (c and d, blue). The merged images of the same view of d were taken by fluorescent microscope (e). Nuclei were stained with Hoechst 33258 (e, blue). Arrows indicate the fused cells. Bars, 100 μm.

fused cells not only expressed cardiac-specific proteins, but also showed the function of cardiomyocytes (i.e., spontaneous beating). Evans et al. (1994) have reported that neonatal cardiomyocyte-fibroblast heterokaryons lose the expression of myosin light chain 2 gene, ANF, and muscle enhancer factor 2 until 6 d, suggesting that the cardiac phenotype is recessive. The discrepancy between our and Evans's results may be explained by the difference in used cells and the method of cell fusion. Evans et al. (1994) used embryonic fibroblasts for coculture and forced the inducing of cell fusion by using polyethylene glycol, whereas we used primary isolated cFB and examined the spontaneous fusion. It remains to be determined whether the nuclei of noncardiomyocytes are reprogrammed to express cardiac proteins by a dominantly acting cardiac factor.

An increase in cardiac mass during fetal period is accomplished predominantly by a cardiomyocyte proliferation, but soon after birth there is a transition from hyperplastic to hypertrophic growth (Morgan and Baker, 1991; Chien, 1995). Many studies have been made to elucidate the mechanism by which cell cycle is arrested in postnatal cardiomyocytes (Agah et al., 1997; Tamamori-Adachi et al., 2003). The adenoviral delivery of cyclinD1 or E2F-1 has been reported to induce cardiomyocytes to reenter the G2/M stage of the cell cycle. In the present work, cardiomyocytes fused with noncardiomyocytes that have proliferative ability expressed G2-M stage cell cycle proteins. After the treatment with nocodazole, PH3-expressing fused cells were significantly enriched, and after the withdrawal of nocodazole, the number was decreased. Moreover, there were fused cells showing the mitotic figures, suggesting that the cell cycle was actively progressing toward the M stage in the fused cells. Engel et al. (2003) have reported that p21 in the cytoplasm of adult cardiomyocytes down-regulates the proliferating cell nuclear antigen protein level in S phase nuclei. The inhibitory effect of the adult cardiomyocyte extract was abolished when an excess volume of S phase cytoplasmic extract from noncardiomyocytes was present. In a similar way, the cytoplasmic factors

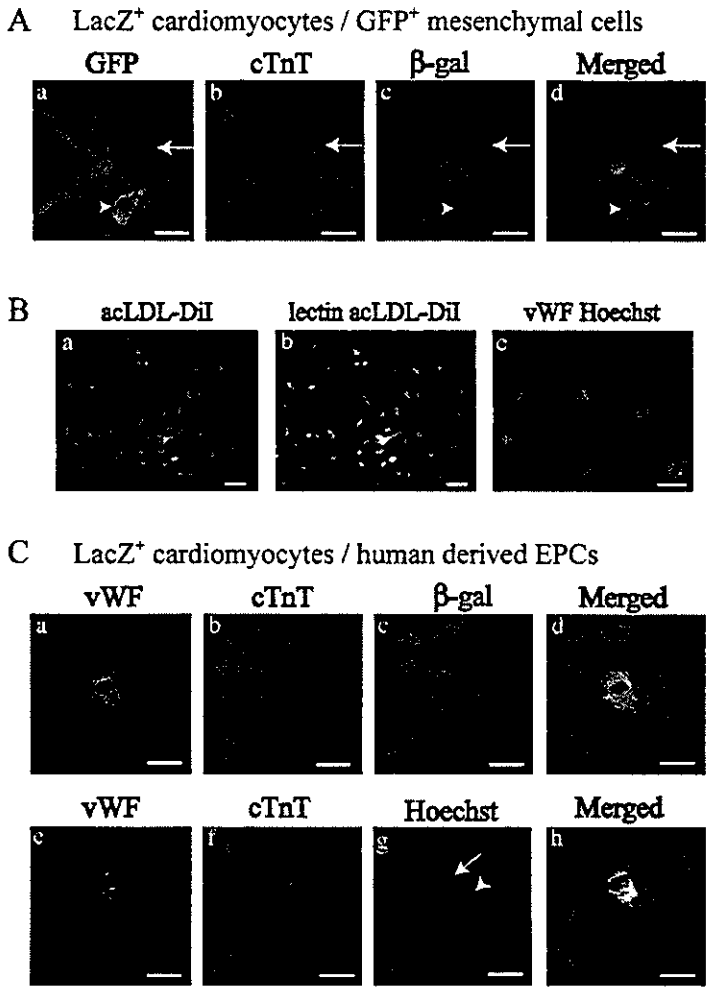

Figure 9. **Cardiomyocytes fused with adult immature somatic cells in vitro.** (A) *LacZ*-expressing cardiomyocytes of neonatal rats were cocultured with GFP+ bone marrow mesenchymal cells. After 4 d of coculture, cells were stained with mouse monoclonal anti-cTnT (red) and rabbit polyclonal anti-β-gal antibodies (blue). Merged image was obtained from the same confocal plane. GFP+ mesenchymal cells (a, arrow) expressed cTnT (b, arrow) and β-gal (c, arrow) in the same cell (merged on d). Arrowheads indicate bone marrow cells fused with noncardiomyocyte. Bars, 50 μm. (B) Fluorescent microscopic images of EPCs cultured 7 d after isolation from peripheral blood. EPCs were identified as double-positive cells of DiI-labeled AcLDL uptake (a, red) and UEA-1 lectin reactivity (b, yellow in merged images). Some adherent cells expressed vWF (c, green). Nuclei were stained with Hoechst 33258 (c, blue). Bars, 50 μm. (C) Human-derived EPCs were cocultured with neonatal mouse cardiomyocytes infected with *LacZ* adenovirus. After 4 d of coculture, cells were stained with rabbit polyclonal anti-vWF (green), goat polyclonal anti-cTnT (red), and mouse monoclonal anti-β-gal antibodies (blue in top row) and Hoechst 33258 (bottom row, blue). The fluorescent confocal microscopic images (a–d, top row) demonstrate that vWF-expressing cells (a) expressed cTnT (b) and β-gal (c) in the same cell. Note that Cy5-conjugated secondary antibodies were used to visualize β-gal. The images of the same cell were taken by fluorescent microscope (e–h, bottom row). Hoechst staining of the nuclei revealed that homogenously stained nuclei (arrow) were of human cell origin and that mouse nuclei showed a punctate appearance (arrowhead). d and h represent merged images. Bars, 50 μm.

of the proliferative cells in the G2-M stage may overcome the unknown endogenous cell cycle inhibitors in the heterokaryons.

We examined two kinds of cells for the in vivo transplantation model. Endothelial cells are a component of the cardiac interstitium, and it is possible that cardiomyocytes fuse with surrounding endothelial cells. Skeletal muscle cells do not exist in the myocardium, but myoblasts have the nature to fuse to form myotubes (Tajbakhsh, 2003), and clinical trials of autologous skeletal myoblast transplantation into the failed heart are currently underway (Menasche et al., 2003; Pagani et al., 2003). Consistent with our in vitro results, cardiomyocytes fused with transplanted HUVEC and skeletal muscle–derived cells. Reinecke et al. (2002) have reported that skeletal myoblasts differentiate into mature skeletal muscle and do not express cardiac-specific genes after been grafted into the heart. In their paper, rat satellite cells were tagged in vitro with BrdU, and the grafted cells were examined by double staining with the BrdU tag and cardiac-specific markers. However, this approach would have disadvantage of potential signal dilution if there is significant donor cell proliferation after transplantation (Dowell et al., 2003). We used genetically modified animals and cells that carry ubiquitously expressed fluorescent proteins or that carry the Cre recombinase gene and the loxP-flanked CAT gene located between CAG promoter and the *LacZ* gene for monitoring donor cell fate after transplantation. These methods possibly enabled us to find rare fused cells in the heart tissue.

In the cryoinjured heart model, some cells in the border zone expressed both cardiomyocyte-specific and endothelial cell–specific proteins. The images were taken with optical sections through an appropriate confocal aperture, so that two different lineage markers were exactly recognized in the same cells. When we cocultured HUVEC with cardiomyocytes, some cells showed transient coexpression of vWF with cardiac sarcomeric proteins (unpublished data). Condorelli et al. (2001) have reported the same findings as a phenomenon that demonstrates the transition from one differentiated state (endothelium) to another (cardiac muscle). Our findings that all cTnT-expressing HUVEC coexpressed cardiomyocyte-derived β-gal and that transplanted HUVEC and cardiomyocytes formed the hybrid cells in the myocardium suggest that the cell fusion of cardiomyocytes with

surrounding endothelial cells occurs in the damaged heart. However, we cannot exclude the possibility of the transdifferentiation of endothelial cells into cardiomyocytes at present. Besides endothelial cells, EPCs have been reported to transdifferentiate into cardiomyocytes in an in vitro coculture model (Badorff et al., 2003). Bone marrow cells have been reported to contain stem cells, which transdifferentiate into various types of cells including vascular cells and cardiomyocytes (Jackson et al., 2001; Orlic et al., 2001a; Jiang et al., 2002). In our work, EPCs and bone marrow–derived mesenchymal cells expressed cardiac-specific proteins through cell fusion with cocultured cardiomyocytes. Therefore, it is possible that circulating EPCs or mesenchymal cells may differentiate into endothelial cells and then fuse with cardiomyocytes. Indeed, recent reports have suggested that transplanted bone marrow–derived cells fuse with preexisting hepatocytes and cardiomyocytes (Alvarez-Dolado et al., 2003; Vassilopoulos et al., 2003; Wang et al., 2003). Recently, cardiac stem cells have been reported to exist in the adult heart (Beltrami et al., 2003; Oh et al., 2003; Matsuura et al., 2004). Sca-1– or c-kit–positive cells from the heart differentiate into cardiomyocytes and other cells including endothelial cells in vitro. Oh et al. (2003) have shown that intravenously infused Sca-1–positive cardiac cells acquire the cardiac phenotypes by both transdifferentiation and fusion, suggesting that cardiac stem cells may differentiate into endothelial cells and then fuse with cardiomyocytes.

In the border zone of rat cryoinjured myocardium, some cardiomyocytes that coexpressed both cTnT and vWF were positively stained with anti-Ki67 antibodies. Ki67 is expressed in all phases of the cell cycle except G0, becomes particularly evident in the late S phase, and is increased further in the G2-M phase. Although Ki67 is not a specific marker for the G2-M stage, Beltrami et al. (2001) have concluded that cardiac myocytes divide in the pathological condition by the evidence of the Ki67 labeling of myocyte nuclei with the mitotic index. We could not detect mitotic figures in the cells that were positively stained with cTnT and vWF, but the expression of Ki67 was observed only in the heterotypic fused cells. Because there were no Ki67-positive nonfused cardiomyocytes, these results suggest that the fused cells enter the cell cycle in vivo as well as in vitro. Wagers and Weissman (2004) have proposed that cell fusion–mediated regeneration might be considered a physiological mechanism of repair. Our results suggest that augmented cell fusion in the diseased heart may contribute to the maintenance and replenishment of cardiomyocytes.

In conclusion, the present work demonstrates that cardiomyocytes have the fusiogenic activity with many different types of cells and obtain proliferative ability after fusion with somatic cells without losing their phenotypes in vitro and in vivo. Our future effort should be toward the understanding of the molecular mechanisms of phenotypic determination and cell cycle activation after fusion. During preparation of this manuscript, Reinecke et al. (2004) have reported that skeletal muscle cell grafting gives rise to skeletal–cardiac hybrid cells with unknown phenotypes. Our findings from the thorough examination of the fused cells are relevant to today's controversy concerning cell plasticity and provide further insights into the understanding of the consequences of cell therapy.

Materials and methods

Animals and reagents

Neonatal (0–1 d old) and adult Wistar rats (8 wk old) were purchased from Takasugi Experimental Animals Supply, Co., Ltd. Adult GFP transgenic mice (Okabe et al., 1997) were gifts from Dr. Okabe (Osaka University, Osaka, Japan). Neonatal and adult GFP transgenic rats (Ito et al., 2001) were purchased from Japan SLC. All protocols were approved by the Institutional Animal Care and Use Committee of Chiba University. The following antibodies were used for immunostaining: mouse monoclonal anti-cTnT (RV-C2, DSMZ-Deutsche Sammlung von Mikroorganismen und Zellkulturen GmbH), goat polyclonal anti-cTnT, goat polyclonal anti-GATA4 (Santa Cruz Biotechnology, Inc.), rabbit polyclonal anti-ANF (Peninsula Laboratories), rabbit polyclonal anti-connexin43 (Zymed Laboratories), rabbit polyclonal anti-desmin, rabbit polyclonal anti-vWF, mouse monoclonal anti–rat Ki67, mouse monoclonal anti–human Ki67 (Dako Cytomation), mouse monoclonal anti-β-gal, rabbit polyclonal anti-β-gal (CHEMICON International, Inc.), mouse monoclonal anti-vimentin, mouse monoclonal anti-Cre (Sigma-Aldrich), rabbit polyclonal anti-PH3 (Upstate Biotechnology), mouse monoclonal anti-cyclinB1 (Neomarkers), and rabbit polyclonal anti-RFP (MBL International Corporation). Fluorescent secondary antibodies were purchased from Jackson ImmunoResearch Laboratories. pLEGFP-N1 and pDsRed2-N1 were purchased from CLONTECH Laboratories. Other reagents not specified were obtained from Sigma-Aldrich.

Cell culture

Neonatal rat cardiomyocytes and neonatal mouse cardiomyocytes were cultured as described previously (Komuro et al., 1990), basically according to the methods of Simpson and Savion (1982). Cardiomyocytes were plated at a field density of 10^5 cells/cm^2 on 35-mm culture dishes containing cover glasses coated by 1% gelatin, and cultured in DME with 10% FBS. cFB were obtained from primary culture described above by preplating technique. Fibroblasts on culture dishes were diluted fourfold, and infected with GFP- or RFP-expressing retroviral vector. Identification and characterization of GFP$^+$ or RFP$^+$ cFB was accomplished by immunocytochemistry and there were not vWF- and cTnT-expressing cells in GFP$^+$ or RFP$^+$ cFB. cFB from passages 3–5 were used. HUVEC were cultured on 0.1% gelatin-coated 100-mm dishes with EGM-2 (Cambrex Bio Science).

Bone marrow mononuclear cells were isolated from 10-wk-old GFP mouse by density gradient centrifugation with Histopaque-1083 as described previously (Zou et al., 2003). Primary culture of the bone marrow cells was performed according to Dexter's method with a few modifications (Dexter et al., 1977). Cells were cultured in Iscove's modified Dulbecco's medium supplemented with 10% FBS at 33°C in humid air with 5% CO_2. After 4 d in culture, nonadherent cells were collected as hematopoietic cells and were used to coculture with cardiomyocytes. Adherent cells were cultured though 14 d and were used to coculture with cardiomyocytes.

Human peripheral mononuclear cells were isolated from blood of human healthy volunteers by density gradient centrifugation with Histopaque-1077. Cells were plated on culture dishes coated with fibronectin in 0.5% gelatin solution and maintained in EGM-2. After 4 d in culture, nonadherent cells were removed by washing with PBS, and the culture was maintained though 7 d. After 7 d in culture, EPCs, recognized as attaching spindle-shaped cells, were assayed by costaining with DiI-labeled AcLDL (Biomedical Technologies) and FITC-labeled UEA-1 lectin. Cells were first incubated with 10 mg/ml DiI-labeled AcLDL at 37°C for 1 h and later fixed with 2% PFA for 10 min. After washes, the cells were reacted with 10 mg/ml FITC-labeled UEA-1 for 1 h. At 7 d in culture, ~30% of cells expressed vWF. Adherent cells at 7 d in culture were used to coculture with cardiomyocytes.

Skeletal muscle–derived cells were isolated from hind limbs of neonatal Sprague-Dawley rats or adult mice as described previously (Iijima et al., 2003). In brief, muscle tissues were minced smaller than 1 mm^3 and digested for a total of 45–60 min of three successive treatments with 0.05% trypsin-EDTA. The cells were collected in the supernatant after each treatment and resuspended in Ham's F10 medium in the presence of 20% horse serum, 0.5% chicken embryo extract, and 2.5 ng/ml bFGF. The cells were grown for 4 d in the same medium on the 2% gelatin-coated dishes. Then the medium was replaced by fresh medium supplemented with 20% FBS and cultured for 2 d.

Labeling of cells

DsRed2 sites of pDsRed2-N1 were subcloned in frame into Xho1 and Not1 sites of pLEGFP-N1 vector. Retroviral stocks were generated as described previously (Minamino et al., 2001). HUVEC and cFB were infected with the GFP- or RFP-expressing retroviral vector. Infected cells were selected for growth in the presence of 500 μg/ml neomycin for 2 wk. The

efficiency of transfection of GFP and RFP was over 95%. Skeletal muscle–derived cells at 4 d after isolation were infected with RFP-expressing retroviral vector. Infected cells were not selected and used for transplantation. The efficiency of transfection of RFP was ~50%.

Neonatal rat cardiomyocytes and neonatal mouse cardiomyocytes were tagged with recombinant adenovirus containing the *Escherichia coli LacZ* gene at a multiplicity of infection of 20 units for 24 h before coculture. After X-gal staining (Minamino et al., 2002), ~100% of cardiomyocytes were recognized to express β-gal.

The adenovirus AxCANCre (RIKEN BRC DNA Bank no. 1748) contains the Cre gene with a nuclear localized signal (NCre) (Kanegae et al., 1995) driven by the CAG promoter (Niwa et al., 1991). HUVEC were infected with AxCANCre at a multiplicity of infection of 50 units for 24 h before the transplantation. After immunostaining, ~100% of HUVEC were recognized to express Cre.

Coculture of neonatal cardiomyocytes with noncardiomyocytes

Neonatal cardiomyocytes were cultured through 4 d and then fluorescence-labeled HUVEC, cFB, bone marrow cells, and nonlabeled EPCs were cultured with cardiomyocytes at a 1:4 ratio. Coculture was maintained in adequate medium for each noncardiomyocyte. Cells were fixed with 4% PFA for 15 min at RT and were subjected to immunostaining at various time points after starting coculture.

Cell transplantation

GFP transgenic adult male rats were anesthetized with ketamine (50 mg/kg, i.p.) and xylazine (10 mg/kg, i.p.). A normal heart was injected with a standard dose of 10^6 RFP-expressing HUVEC or skeletal muscle–derived cells (Reinecke and Murry, 2003). In the HUVEC transplantation model, the immunosupressor FK506 (Fujisawa Pharmaceutical) was administered i.p. at 2.0 mg/kg body weight on the day of injection and maintained until the animals were killed. The hearts were fixed according to the periodate–lysine–PFA fixative methods and were snap-frozen in nitrogen and stored for subsequent immunohistochemical analysis.

MerCreMer mice express MerCreMer fusion protein driven by the αMHC promoter (Sohal et al., 2001). CAG-CAT-*LacZ* transgenic mice direct expression of the *E. coli LacZ* gene upon Cre-mediated excision of the loxP-flanked CAT gene located between the CAG promoter and the *LacZ* gene (Sakai and Miyazaki, 1997; Dr. Miyazaki, Osaka University, Osaka, Japan). A dose of 10^6 Cre-expressing HUVEC were transplanted to the heart of CAG-CAT-*LacZ* transgenic mice with the i.p. administration of FK506 at 2.0 mg/kg body weight on the day of injection and maintained until the animals were killed. A dose of 10^6 skeletal muscle–derived cells isolated from CAG-CAT-*LacZ* transgenic mice were transplanted to the heart of MerCreMer mice. MerCreMer mice were treated with tamoxifen (20 mg/kg/day, i.p.) 7 d before transplantation and the treatment was maintained until 2 d before the transplantation. At 4 d after transplantation, mice were killed and the hearts were perfused with 2% PFA and were snap-frozen in nitrogen. A couple of adjacent sections as a mirror image were prepared and fixed with 0.25% glutaraldehyde or 2% PFA for 15 min and were analyzed by X-gal staining or immunohistochemistry.

Cryoinjury

Male Wistar rats were anesthetized with ketamine (50 mg/kg, i.p.) and xylazine (10 mg/kg, i.p.) and a 6-mm aluminum rod, cooled to −190°C by immersion in liquid nitrogen applied to the left ventricular free wall to produce cryoinjury. The rats were killed at 4 d after cryoinjury. The hearts were snap-frozen in nitrogen. A couple of adjacent sections as a mirror image were prepared and fixed with 4% PFA and were subjected to immunostaining.

Immunohistochemistry

Fixed cells were preblocked with PBS containing 2% donkey serum, 2% BSA, and 0.2% NP-40 for 30 min. Primary antibodies were diluted with PBS containing 2% donkey serum, 2% BSA, and 0.1% NP-40 and applied over night at 4°C. FITC-, Cy3-, or Cy5-conjugated secondary antibodies were applied to visualize expression of specific proteins. Before mounting, nuclei were stained with Hoechst 33258 (1 μg/ml) or Topro3 (Molecular Probes, Inc.). Images of samples were taken by laser confocal microscopy (Radiance 2000; Bio-Rad Laboratories) or with a fluorescent microscope (Carl Zeiss MicroImaging, Inc.) equipped with a CCD camera (Axiocam; Carl Zeiss MicroImaging, Inc.).

Nocodazole treatment and cell cycle analysis

Neonatal rat cardiomyocytes fused with GFP$^+$ HUVEC or GFP$^+$ cFB were treated with 50 ng/ml nocodazole for 6–24 h and at each time cells were fixed and stained with anti-cTnT and anti-PH3 antibodies. Some of the cells treated with nocodazole for 6 h cocultured with HUVEC and for 24 h cocultured with cFB were released from nocodazole and cultured further for 3 h and fixed.

Statistical analysis

Values are presented as mean ± SD. The significance of differences among mean values was determined by one-factor ANOVA, chi-square independent test, and Kruskal-Wallis test. Probability (P) values were corrected for multiple comparisons by the Bonferroni correction. The accepted level of significance was $P < 0.05$.

Online supplemental material

Live images of beating cells were obtained with an inverted microscope (Carl Zeiss MicroImaging, Inc.) equipped with a chilled CCD camera (Hamamatsu Corporation) using I-O DATA Videorecorder software. Online supplemental material available at http://www.jcb.org/cgi/content/full/jcb.200312111/DC1.

We thank M. Watanabe, R. Kobayashi, E. Fujita, A. Furuyama, M. Iida, and Y. Ohtsuki for their excellent technical assistance. We thank Dr. Okabe for GFP transgenic mice and rats, Dr. Miyazaki for CAG-CAT-*LacZ* mice and adenovirus containing the nuclear localized Cre recombinase gene.

This work was supported by a Grant-in-Aid for Scientific Research, Developmental Scientific Research, and Scientific Research on Priority Areas from the Ministry of Education, Science, Sports, and Culture; Takeda Medical Research Foundation; Uehara Memorial Foundation; Grant-in-Aid of The Japan Medical Association; The Kato Memorial Trust for Nambyo Research; and Takeda Science Foundation.

Submitted: 15 December 2003
Accepted: 8 September 2004

References

Agah, R., L.A. Kirshenbaum, M. Abdellatif, L.D. Truong, S. Chakraborty, L.H. Michael, and M.D. Schneider. 1997. Adenoviral delivery of E2F-1 directs cell cycle reentry and p53-independent apoptosis in postmitotic adult myocardium in vivo. *J. Clin. Invest.* 100:2722–2728.

Alvarez-Dolado, M., R. Pardal, J.M. Garcia-Verdugo, J.R. Fike, H.O. Lee, K. Pfeffer, C. Lois, S.J. Morrison, and A. Alvarez-Buylla. 2003. Fusion of bone marrow-derived cells with Purkinje neuron, cardiomyocytes and hepatocytes. *Nature.* 425:968–973.

Badorff, C., R.P. Brandes, R. Popp, S. Rupp, C. Urbich, A. Aicher, I. Fleming, R. Busse, A.M. Zeiher, and S. Dimmeler. 2003. Transdifferentiation of blood-derived human adult endothelial progenitor cells into functionally active cardiomyocytes. *Circulation.* 107:1024–1032.

Baron, M.H. 1993. Reversibility of the differentiated state in somatic cells. *Curr. Opin. Cell Biol.* 5:1050–1056.

Beltrami, A.P., K. Urbanek, J. Kajstura, S.M. Yan, N. Finato, R. Bussani, B. Nadal-Ginard, F. Silvestri, A. Leri, C.A. Beltrami, and P. Anversa. 2001. Evidence that human cardiac myocytes divide after myocardial infarction. *N. Engl. J. Med.* 344:1750–1757.

Beltrami, A.P., L. Barlucchi, D. Torella, M. Baker, F. Limana, S. Chimenti, H. Kasahara, M. Rota, E. Musso, K. Urbanek, et al. 2003. Adult cardiac stem cells are multipotent and support myocardial regeneration. *Cell.* 114:763–776.

Blajeski, A.L., V.A. Phan, T.J. Kottke, and S.H. Kaufmann. 2002. G_1 and G_2 cell-cycle arrest following microtubule depolymerization in human breast cancer cells. *J. Clin. Invest.* 110:91–99.

Blau, H.M., C.P. Chiu, and C. Webster. 1983. Cytoplasmic activation of human nuclear genes in stable heterocaryons. *Cell.* 32:1171–1180.

Blau, H.M., and B.T. Blakely. 1999. Plasticity of cell fate: insights from heterokaryons. *Semin. Cell Dev. Biol.* 10:267–272.

Chien, K.R. 1995. Cardiac muscle diseases in genetically engineered mice: evolution of molecular physiology. *Am. J. Physiol.* 269:H755–H766.

Condorelli, G., U. Borello, L. De Angelis, M. Latronico, D. Sirabella, M. Coletta, R. Galli, G. Balconi, A. Follenzi, G. Frati, et al. 2001. Cardiomyocytes induce endothelial cells to trans-differentiate into cardiac muscle: implications for myocardium regeneration. *Proc. Natl. Acad. Sci. USA.* 98:10733–10738.

Dexter, T.M., T.D. Allen, and L.G. Lajtha. 1977. Conditions controlling the proliferation of haemopoietic stem cells in vitro. *J. Cell. Physiol.* 91:335–344.

Dowell, J.D., M. Rubart, K.B. Pasumarthi, M.H. Soonpaa, and L.J. Field. 2003. Myocyte and myogenic stem cell transplantation in the heart. *Cardiovasc. Res.* 58:336–350.

Engel, F.B., L. Hauck, M. Boehm, E.G. Nabel, R. Dietz, and R. von Harsdorf. 2003. $p21^{CIP1}$ controls proliferating cell nuclear antigen level in adult cardiomyocytes. *Mol. Cell. Biol.* 23:555–565.

Evans, S.M., L.J. Tai, V.P. Tan, C.B. Newton, and K.R. Chien. 1994. Heterokaryons of cardiac myocytes and fibroblasts reveal the lack of dominance of the cardiac muscle phenotype. *Mol. Cell. Biol.* 14:4269–4279.

Iijima, Y., T. Nagai, M. Mizukami, K. Matsuura, T. Ogura, H. Wada, H. Toko, H. Akazawa, H. Takano, H. Nakaya, and I. Komuro. 2003. Beating is necessary for transdifferentiation of skeletal muscle-derived cells into cardiomyocytes. *FASEB J.* 17:1361–1363.

Ito, T., A. Suzuki, E. Imai, M. Okabe, and M. Hori. 2001. Bone marrow is a reservoir of repopulating mesangial cells during glomerular remodeling. *J. Am. Soc. Nephrol.* 12:2625–2635.

Jackson, K.A., S.M. Majka, H. Wang, J. Pocius, C.J. Hartley, M.W. Majesky, M.L. Entman, L.H. Michael, K.K. Hirschi, and M.A. Goodell. 2001. Regeneration of ischemic cardiac muscle and vascular endothelium by adult stem cells. *J. Clin. Invest.* 107:1395–1402.

Jiang, Y., B.N. Jahagirdar, R.L. Reinhardt, R.E. Schwartz, C.D. Keene, X.R. Ortiz-Gonzalez, M. Reyes, T. Lenvik, T. Lund, M. Blackstad, et al. 2002. Pluripotency of mesenchymal stem cells derived from adult marrow. *Nature.* 418:41–49.

Kajstura, J., A. Leri, N. Finato, C. Di Loreto, C.A. Beltrami, and P. Anversa. 1998. Myocyte proliferation in end-stage cardiac failure in human. *Proc. Natl. Acad. Sci. USA.* 95:8801–8805.

Kalka, C., H. Masuda, T. Takahashi, W.M. Kalka-Moll, M. Silver, M. Kearney, T. Li, J.M. Isner, and T. Asahara. 2000. Transplantation of ex vivo expanded endothelial progenitor cells for therapeutic neovascularization. *Proc. Natl. Acad. Sci. USA.* 97:3422–3427.

Kanegae, Y., G. Lee, Y. Sato, M. Tanaka, M. Nakai, T. Sakaki, S. Sugano, and I. Saito. 1995. Efficient gene activation in mammalian cells by using recombinant adenovirus expressing site-specific Cre recombinase. *Nucleic Acids Res.* 23:3816–3821.

Komuro, I., T. Kaida, Y. Shibazaki, M. Kurabayashi, Y. Katoh, E. Hoh, F. Takaku, and Y. Yazaki. 1990. Stretching cardiac myocytes stimulates protooncogene expression. *J. Biol. Chem.* 265:3595–3598.

Mangi, A.A., N. Noiseux, D. Kong, H. He, M. Rezvani, J.S. Ingwall, and V.J. Dzau. 2003. Mesenchymal stem cells modified with Akt prevent remodeling and restore performance of infarcted hearts. *Nat. Med.* 9:1195–1201.

Matsuura, K., T. Nagai, N. Nishigaki, T. Oyama, J. Nishi, H. Wada, M. Sano, H. Toko, H. Akazawa, T. Sato, et al. 2004. Adult cardiac Sca-1-positive cells differentiate into beating cardiomyocytes. *J. Biol. Chem.* 279: 11384–11391.

Menasche, P., A.A. Hagege, J.T. Vilquin, M. Desnos, E. Abergel, B. Pouzet, A. Bel, S. Sarateanu, M. Scorsin, K. Schwartz, et al. 2003. Autologous skeletal myoblast transplantation for severe postinfarction left ventricular dysfunction. *J. Am. Coll. Cardiol.* 41:1078–1083.

Minamino, T., S.A. Mitsialis, and S. Kourembanas. 2001. Hypoxia extends the life span of vascular smooth muscle cells through telomerase activation. *Mol. Cell. Biol.* 21:3336–3342.

Minamino, T., H. Miyauchi, T. Yoshida, Y. Ishida, H. Yoshida, and I. Komuro. 2002. Endothelial cell senescence in human atherosclerosis: role of telomere in endothelial dysfunction. *Circulation.* 105:1541–1544.

Morgan, H.E., and K.M. Baker. 1991. Cardiac hypertrophy. *Circulation.* 83: 13–25.

Niwa, H., K. Yamamura, and J. Miyazaki. 1991. Efficient selection for high-expression transfectants with a novel eukaryotic vector. *Gene.* 108:193–200.

Oh, H., S.B. Bradfute, T.D. Gallardo, T. Nakamura, V. Gaussin, Y. Mishina, J. Pocius, L.H. Michael, R.R. Behringer, D.J. Garry, et al. 2003. Cardiac progenitor cells from adult myocardium: homing, differentiation, and fusion after infarction. *Proc. Natl. Acad. Sci. USA.* 100:12313–12318.

Okabe, M., M. Ikawa, K. Kominami, T. Nakanishi, and Y. Nishimune. 1997. "Green mice" as a source of ubiquitous green cells. *FEBS Lett.* 407: 313–319.

Orlic, D., J. Kajstura, S. Chimenti, I. Jakoniuk, S.M. Anderson, B. Li, J. Pickel, R. McKay, B. Nadal-Ginard, D.M. Bodine, et al. 2001a. Bone marrow cells regenerate infarcted myocardium. *Nature.* 410:701–705.

Orlic, D., J. Kajstura, S. Chimenti, F. Limana, I. Jakoniuk, F. Quaini, B. Nadal-Ginard, D.M. Bodine, A. Leri, and P. Anversa. 2001b. Mobilized bone marrow cells repair the infracted heart, improving function and survival. *Proc. Natl. Acad. Sci. USA.* 98:10344–10349.

Pagani, F.D., H. DerSimonian, A. Zawadzka, K. Wetzel, A.S. Edge, D.B. Jacoby, J.H. Dinsmore, S. Wright, T.H. Aretz, H.J. Eisen, and K.D. Aaronson. 2003. Autologous skeletal myoblasts transplanted to ischemia-damaged myocardium in humans. Histological analysis of cell survival and differentiation. *J. Am. Coll. Cardiol.* 41:879–888.

Reinecke, H., and C.E. Murry. 2003. Cell grafting for cardiac repair. *Methods Mol. Biol.* 219:97–112.

Reinecke, H., V. Poppa, and C.E. Murry. 2002. Skeletal muscle stem cells do not transdifferentiate into cardiomyocytes after cardiac grafting. *J. Mol. Cell. Cardiol.* 34:241–249.

Reinecke, H., E. Minami, V. Poppa, and C.E. Murry. 2004. Evidence for fusion between cardiac and skeletal muscle cells. *Circ. Res.* 94:e56–e60.

Sakai, K., and J. Miyazaki. 1997. A transgenic mouse line that retains Cre recombinase activity in mature oocytes irrespective of the cre transgene transmission. *Biochem. Biophys. Res. Commun.* 237:318–324.

Simpson, P., and S. Savion. 1982. Differentiation of rat myocytes in single cell cultures with and without proliferative nonmyocardial cells. Cross-striations, ultrastructure, and chronotropic response to isoproterenol. *Circ. Res.* 50:101–116.

Sohal, D.S., M. Nghiem, M.A. Crackower, S.A. Witt, T.R. Kimball, K.M. Tymitz, J.M. Penninger, and J.D. Molkentin. 2001. Temporally regulated and tissue-specific gene manipulations in the adult and embryonic heart using a tamoxifen-inducible Cre protein. *Circ. Res.* 89:20–25.

Tajbakhsh, S. 2003. Stem cells to tissue: molecular, cellular and anatomical heterogeneity in skeletal muscle. *Curr. Opin. Genet. Dev.* 13:413–422.

Tamamori-Adachi, M., H. Ito, P. Sumrejkanchanakij, S. Adachi, M. Hiroe, M. Shimizu, J. Kawauchi, M. Sunamori, F. Marumo, S. Kitajima, and M.A. Ikeda. 2003. Critical role of cyclin D1 nuclear import in cardiomyocyte proliferation. *Circ. Res.* 92:e12–e19.

Terada, N., T. Hamazaki, M. Oka, M. Hoki, D.M. Mastalerz, Y. Nakano, E.M. Meyer, L. Morel, B.E. Petersen, and E.W. Scott. 2002. Bone marrow cells adopt the phenotype of other cells by spontaneous cell fusion. *Nature.* 416:542–545.

Vassilopoulos, G., P.R. Wang, and D.W. Russell. 2003. Transplanted bone marrow regenerates liver by cell fusion. *Nature.* 422:901–904.

Wagers, A.J., and I.L. Weissman. 2004. Plasticity of adult stem cells. *Cell.* 116: 639–648.

Wang, X., H. Willenbring, Y. Akkari, Y. Torimaru, M. Foster, M. Al-Dhalimy, E. Lagasse, M. Finegold, S. Olson, and M. Grompe. 2003. Cell fusion is the principal source of bone-marrow-derived hepatocytes. *Nature.* 422: 897–901.

Weimann, J.M., C.B. Johansson, A. Trejo, Y., and H.M. Blau. 2003. Stable reprogrammed heterokaryons form spontaneously in Purkinje neurons after bone marrow transplant. *Nat. Cell Biol.* 5:959–966.

Ying, Q.L., J. Nichols, E.P. Evans, and A.G. Smith. 2002. Changing potency by spontaneous fusion. *Nature.* 416:545–548.

Zou, Y., H. Takano, M. Mizukami, H. Akazawa, Y. Qin, H. Toko, M. Sakamoto, T. Minamino, T. Nagai, and I. Komuro. 2003. Leukemia inhibitory factor enhances survival of cardiomyocytes and induces regeneration of myocardium after myocardial infarction. *Circulation.* 108:748–753.

THE JOURNAL OF CELL BIOLOGY

Katsuhisa Matsuura, Hiroshi Wada, Toshio Nagai, Yoshihiro Iijima, Tohru Minamino, Masanori Sano, Hiroshi Akazawa, Jeffery D. Molkentin, Hiroshi Kasanuki, and Issei Komuro

Vol. 167, No. 2, October 25, 2004. Pages 351–363.

A label (RFP$^+$ HUVEC) was left out of figure 2 B. The corrected figure appears below.

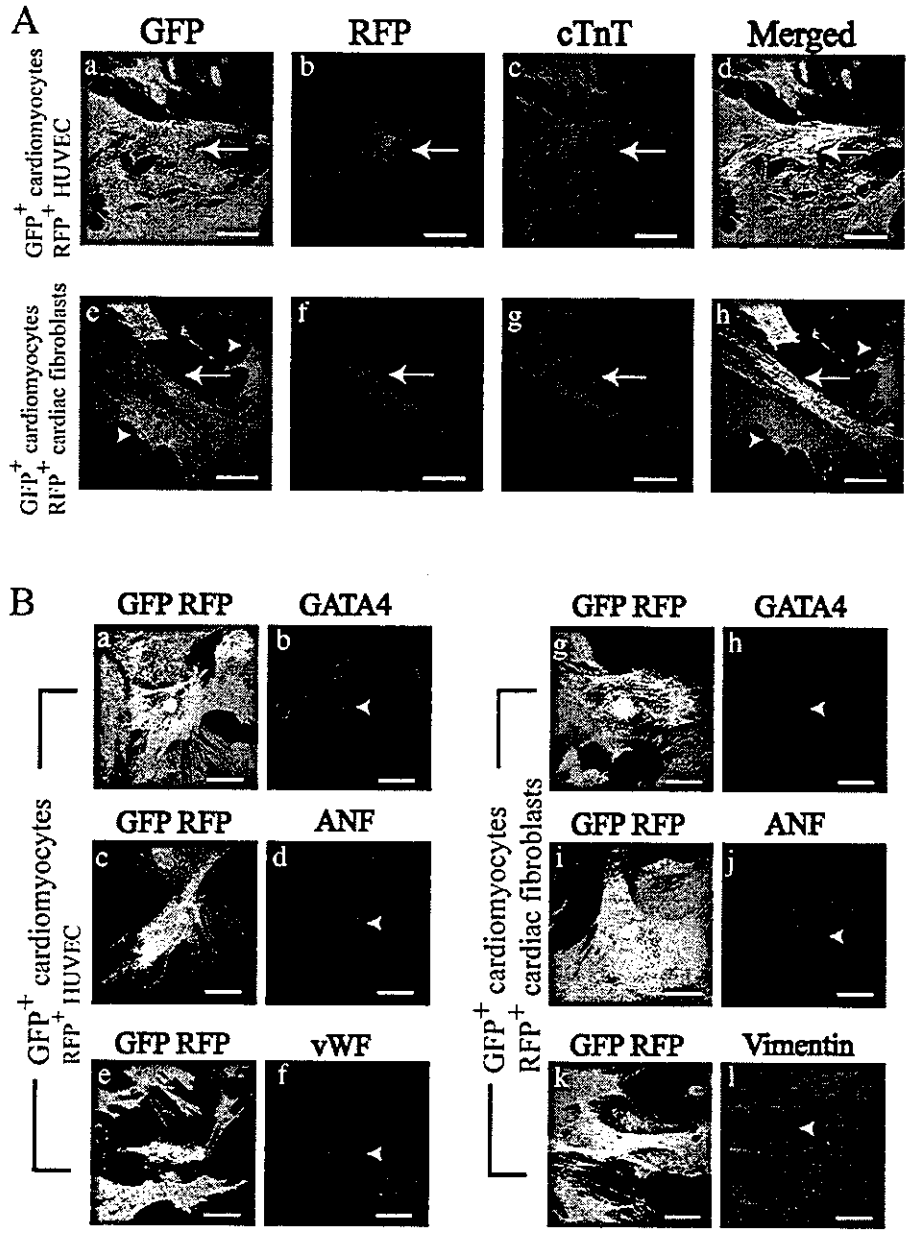

Available online at www.sciencedirect.com
SCIENCE DIRECT®
Biochemical and Biophysical Research Communications 325 (2004) 1353–1359
BBRC
www.elsevier.com/locate/ybbrc

Effects of G-CSF on cardiac remodeling after acute myocardial infarction in swine

Koji Iwanaga[a], Hiroyuki Takano[a], Masashi Ohtsuka[a], Hiroshi Hasegawa[a], Yunzeng Zou[a], Yingjie Qin[a], Kenichi Odaka[a], Kenzo Hiroshima[b], Hiroyuki Tadokoro[c], Issei Komuro[a,*]

[a] *Department of Cardiovascular Science and Medicine, Chiba University Graduate School of Medicine, Chiba, Japan*
[b] *Department of Basic Pathology, Chiba University Graduate School of Medicine, Chiba, Japan*
[c] *Division of Medical Imaging, National Institute of Radiological Science, Chiba, Japan*

Received 19 October 2004
Available online 11 November 2004

Abstract

We examined whether granulocyte colony-stimulating factor (G-CSF) prevents cardiac dysfunction and remodeling after myocardial infarction (MI) in large animals. MI was produced by ligation of left anterior descending coronary artery in swine. G-CSF (10 μg/kg/day, once a day) was injected subcutaneously from 24 h after ligation for 7 days. Echocardiographic examination revealed that the G-CSF treatment induced improvement of cardiac function and attenuation of cardiac remodeling at 4 weeks after MI. In the ischemic region, the number of apoptotic endothelial cells was smaller and the number of vessels was larger in the G-CSF treatment group than in control group. Moreover, vascular endothelial growth factor was more abundantly expressed and Akt was more strongly activated in the ischemic region of the G-CSF treatment group than of control group. These findings suggest that G-CSF prevents cardiac dysfunction and remodeling after MI in large animals.

Keywords: Akt; Angiogenesis; Apoptosis; Cytokine; G-CSF; Myocardial infarction; Remodeling; Swine; VEGF

Since left ventricular (LV) remodeling after myocardial infarction (MI) causes progression to heart failure, preventing the remodeling process following MI is an important therapeutic approach for heart failure. Although the therapeutic agents such as angiotensin converting enzyme inhibitors and β blockers prevent cardiac remodeling and reduce morbidity and mortality in patients with heart failure after MI, loss of cardiac myocytes could not be prevented by these agents. Although cardiac myocytes were previously considered as terminally differentiated cells, it has been recently reported that there are proliferating cardiac myocytes after MI in human hearts [1]. Moreover, it has been demonstrated that bone marrow stem cells (BMSCs) differentiate into cardiac myocytes, endothelial cells (ECs), and vascular smooth muscle cells (VSMCs) in adult mouse model of MI [2]. A highly enriched hematopoietic stem cell (HSC) population, so-called side population (SP), has also been reported to have the capacity to regenerate cardiac myocytes and blood vessels [3]. These studies suggest that locally delivered BMSCs or engrafted SP cells may generate new myocardium and then improve prognosis of patients with MI.

Granulocyte colony-stimulating factor (G-CSF) causes a marked increase in the release of HSCs and endothelial progenitor cells (EPCs) from bone marrow (BM) into the peripheral blood circulation, a process termed mobilization [4–7]. Recently, it has been reported that G-CSF improves cardiac function and reduces mortality after MI in mice [6–8]. The mobilized BM cells have been reported to differentiate into cardiac

* Corresponding author. Fax: +81 43 226 2557.
E-mail address: komuro-tky@umin.ac.jp (I. Komuro).

0006-291X/S - see front matter © 2004 Elsevier Inc. All rights reserved.
doi:10.1016/j.bbrc.2004.10.149

myocytes, ECs, and VSMCs [6]. However, there have been reports indicating that transdifferentiation of BM cells into cardiomyocytes is very rare [7,8]. Thus, mechanisms by which G-CSF ameliorates cardiac dysfunction are not fully understood. In the present study, we examined as a preclinical study whether G-CSF treatment is effective in preventing cardiac remodeling after MI also in large animals and investigated the mechanism of beneficial effects of G-CSF.

Materials and methods

Swine MI model. Male Yorkshire swine (Science Breeding Farm, Iwate, Japan) weighing 15–20 kg were used to induce myocardial infarction. After opening the chest, permanent occlusion was created between the first and second diagonal branches of the left anterior descending coronary artery (LAD) with a 3-0 nylon surgical suture. The mortality during operation was approximately 20% in this study. All the cause of death was arrhythmia (ventricular tachycardia and ventricular fibrillation). Since we used the swine which had not suffered arrhythmia, the swine were not treated with electrical defibrillation. All protocol was approved by the Institutional Animal Care and Use Committee of the Chiba University.

Cytokine treatment. The swine were randomized into two groups. (1) G-CSF treatment group ($n = 10$); injected subcutaneously with recombinant human G-CSF (10 μg/kg/day, Kirin Brewery, Tokyo, Japan). (2) control group ($n = 10$); injected subcutaneously with saline as the same volume as G-CSF, beginning at 24 h after MI and continuning daily for 7 days. The numbers of circulating white blood cells (WBC) and granulocytes were counted before and at 1, 3, 5, 7, and 28 days after MI. By using myocardial contrast echocardiography (MCE) analysis, we confirmed every time before the permanent ligation of LAD that the extent of area at risk (AAR) was constant. After that, an investigator, who was different from operators, randomized the swine into two groups. The measurement of echocardiography and the estimation of pathology were performed by other persons blinded to randomization. Moreover, we measured the serum levels of creatine kinase-MB isoenzyme (CK-MB) and cardiac troponin I (cTnI) at the earlier time points after MI in both G-CSF treatment group and control group.

Physiological analysis. Echocardiographic studies were performed at pre-operation and 4 weeks after LAD ligation with an Philips Sonos 5500 and an ultraband S4 sector transducer. The transducer was placed on a standoff positioned on the epicardium. LV end-diastolic area (LVAd), LV end-systolic area (LVAs), diastolic interventricular septum wall thickness (IVSTd), diastolic LV posterior wall thickness (PWTd), and fractional area change (FAC) at the level of mid papillary muscles in short-axis view were measured by B-mode. MCE was performed with contrast agent (Levovist, Nihon Schering, 300 mg/10 s).

Histological analysis. Four weeks after MI, triphenyltetrazolium chloride (TTC) staining was performed to estimate infarct size. The heart was cut into six transverse slices, and one slice containing the mid papillary muscle was incubated for 5 min at 37 °C in 1% solution of TTC. The infarcted (pale) and viable (red) myocardium were measured by computed planimetry (NIH IMAGE 1.63, NIH, ML). Infarct size measured from tracing of myocardial slices was calculated as a percentage of LV area. Cardiomyocytes were identified immunohistochemically using anti-cardiac troponin T (cTnT) antibody (Santa Cruz Biotechnology, CA). Endothelial cells were identified immunohistochemically using anti-von Willebrand factor (vWF) antibody (Dako, CA) and smooth muscle cells were identified by anti-α-smooth muscle actin antibody (Dako, CA). Expressions of cTnT and vWF were visualized by Cy3-labeled secondary antibody. To count the numbers of vessels, 15 fields were randomly chosen from remote (non-infarct), border (ischemia), and infarct regions in each sample ($n = 10$, each groups). For detection of apoptotic cells, TUNEL assay was performed using In situ Apoptosis Detection Kit (Takara, Japan). To identify which cells were TUNEL-positive, we further performed double-staining by using anti-cTnT or anti-vWF antibody with TUNEL assay.

Western blot analysis. Four weeks after MI, whole tissue lysates were extracted from hearts and subjected to Western blot analysis. The extracts were centrifuged at 14,000 rpm at 4 °C for 30 min, and the total protein concentration was measured with the BCA protein assay kit (Pierce, IL). Proteins (50 μg) were separated in 10–15% SDS–PAGE and transferred onto a nitrocellulose transfer membrane (Schleicher & Schuell, Netherlands). After blocking in TBS-T (150 mmol/L NaCl, 50 mmol/L Tris, and 0.1% Tween 20, pH 7.4) containing 5% skim milk, the membranes were incubated with antibodies against Akt1, phospho-Akt1, or VEGF (Santa Cruz Biotechnology, CA). VEGF blocking peptide was used to identify the band of VEGF. Hybridizing bands were visualized using an ECL detecting kit (Amersham–Pharmacia Biotech, NJ). The equal loading was validated by staining with Ponceau S.

Statistical analysis. All data are presented as means ± SD. All data were analyzed by one-way ANOVA followed by the Bonferroni procedure for comparison of means. A probability value of $P < 0.05$ was considered to be statistically significant.

Results

Blood collection and laboratory analysis

Blood samples were collected before and at 1, 3, 5, 7, and 28 days after MI with or without G-CSF treatment (Figs. 1A and B). Although there was no significant difference in their numbers between G-CSF treatment group and control group at pre-operation, both numbers were significantly larger in G-CSF treatment group (WBC, $55{,}500 \pm 16{,}426/mm^3$; granulocytes, $41{,}352 \pm 14{,}791/mm^3$) than in control group (WBC, $21{,}000 \pm 7867/mm^3$, granulocytes, $10{,}932 \pm 6827/mm^3$) at 3 days after MI (Figs. 1A and B). Plasma G-CSF concentration was not detectable at pre-operation in both groups and was increased at 1 week after MI in control group (192 ± 1.4 pg/mL). G-CSF concentration was much higher in G-CSF treatment group (1980 ± 867 pg/mL) than in control group, suggesting that subcutaneously injected G-CSF (10 μg/kg/day) was enough to induce mobilization in swine model. We next evaluated the size of infarction in both groups by measuring the serum levels of CK-MB and cTnI. Since there were no significant differences in the levels of CK-MB and cTnI between control group and the G-CSF treatment group at the any time after MI, the initial infarct size of both groups seemed to be same (Figs. 1C and D).

Echocardiographic analysis

We evaluated cardiac function and LV remodeling by echocardiography at pre-operation and 4 weeks after MI (Table 1). At pre-operation there was no significant

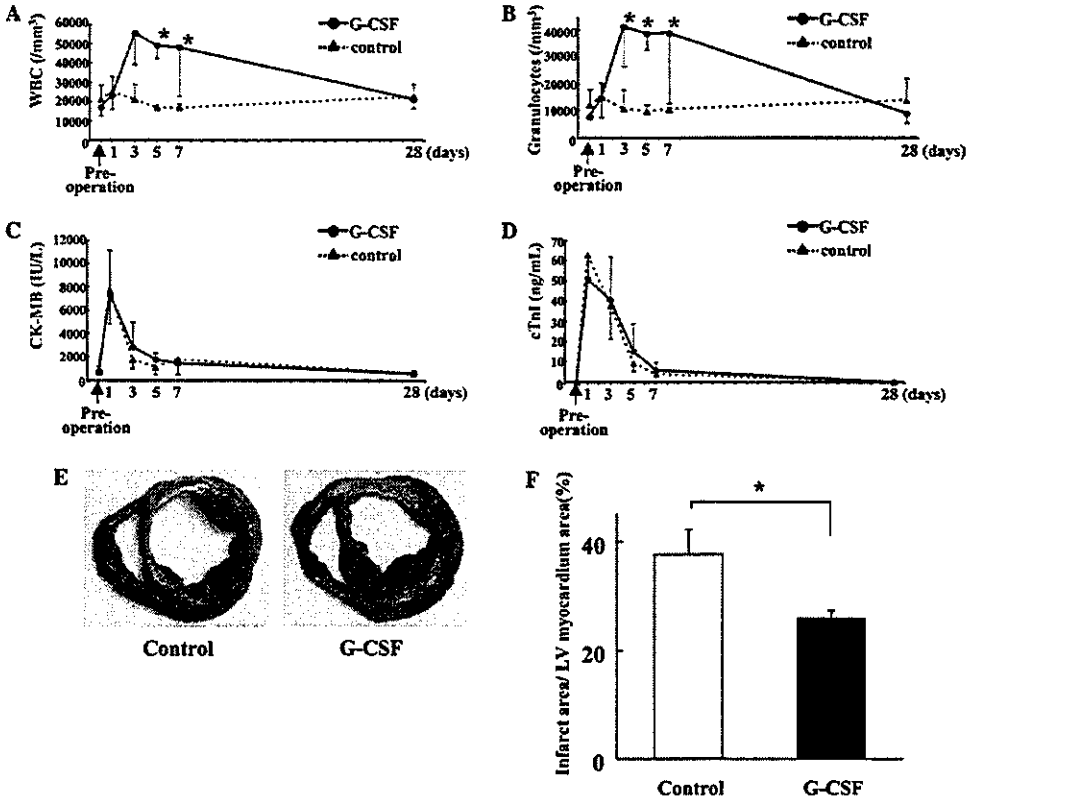

Fig. 1. Histological analysis. (A,B) The number of circulating white blood cells (WBC) and granulocytes was counted at pre-operation, 1, 3, 5, 7, and 28 days after MI. (C) Serum levels of creatine kinase-MB isozyme (CK-MB) were measured at pre-operation, 1, 3, 5, 7, and 28 days after MI. (D) Serum levels of cardiac troponin I (cTnI) were measured at pre-operation, 1, 3, 5, 7, and 28 days after MI. There was no significant difference in CK-MB and cTnI levels between control group and the G-CSF treatment group at any time after MI. (E) Triphenyltetrazolium chloride (TTC) staining. The area of infarcted (pale) and viable (red) myocardium was measured by computed planimetry. (F) Infarct size measured from tracing of myocardial slices was calculated as a percentage of LV area. Infarct size was much smaller in the G-CSF treatment group than in control group. Results are given as means ± SD ($n = 10$). $^*P < 0.05$.

Table 1
Echocardiographic parameters measured before and 4 weeks after MI

	IVSTd (mm)		PWTd (mm)		LVAd (cm^2)		LVAs (cm^2)		FAC (%)	
	Pre-MI	4w	Pre-MI	4w	Pre-MI	4w	Pre-MI	4w	Pre-MI	4w
Control	6.1 ± 1.1	3.5 ± 0.4	6.3 ± 0.8	7.5 ± 1.0	8.1 ± 1.0	17.6 ± 2.1	5.1 ± 0.7	12.4 ± 2.9	37.5 ± 8.0	18.1 ± 4.0
G-CSF	6.1 ± 1.1	5.1 ± 1.0*	6.4 ± 0.9	6.3 ± 0.9*	8.4 ± 1.4	12.5 ± 1.7*	5.1 ± 0.9	8.1 ± 0.6*	38.7 ± 10.7	29.6 ± 5.4*

IVSTd, interventricular septum wall thickness at diastole; PWTd, LV posterior wall thickness at diastole; LVAd, LV end-diastolic area; LVAs, LV end-systolic area; and FAC, fractional area change.
* $P < 0.05$ vs control.

difference in cardiac performance between control group (IVSTd, 6.1 ± 1.1 mm; PWTd, 6.3 ± 0.8 mm; LVAd, 8.1 ± 1.0 cm^2; LVAs, 5.1 ± 0.7 cm^2; and FAC, 37.5 ± 8.0%) and the G-CSF-treatment group (IVSTd, 6.1 ± 1.1 mm; PWTd, 6.4 ± 0.9 mm; LVAd, 8.4 ± 1.4 cm^2; LVAs, 5.1 ± 0.9 cm^2; and FAC, 38.7 ± 10.7%). The change of these parameters became more prominent in control group at 4 weeks after MI (IVSTd, 3.5 ± 0.4 mm; PWTd, 7.5 ± 1.0 mm; LVAd, 17.6 ± 2.1 cm^2; LVAs, 12.4 ± 2.9 cm^2; and FAC, 18.1 ± 4.0%) but not in the G-CSF group (IVSTd, 5.1 ± 1.0 mm; PWTd, 6.3 ± 0.9 mm; LVAd, 12.5 ± 1.7 cm^2; LVAs, 8.1 ± 0.6 cm^2; and FAC, 29.6 ± 5.4%) (Table 1).

Infarct size

Gross anatomical examination revealed that the LV wall thickness at MI region was very thin and the LV

cavity was markedly expanded in control group but not the G-CSF treatment group. TTC staining revealed that infarct area/LV myocardium area (%) was significantly less in the G-CSF treatment group than in control group (Figs. 1E and F).

Neovascularization

To clarify the mechanisms by which G-CSF improves LV remodeling and dysfunction after MI, we first examined the number of vessels because it has been reported that injection of BM cells into the heart after MI prevents the remodeling through angiogenesis and that G-CSF induces mobilization of EPCs [6–9]. In both border and infarct regions, there were more vWF-positive vessels in the G-CSF treatment group than in control group (Figs. 2A and B). These results suggest that G-CSF may ameliorate myocardial perfusion at least in part through an increase in the numbers of vessels.

Apoptotic cells

It has been reported that apoptotic cell death contributes to expansion of MI extent and progression of LV remodeling after MI [10]. We thus measured the number

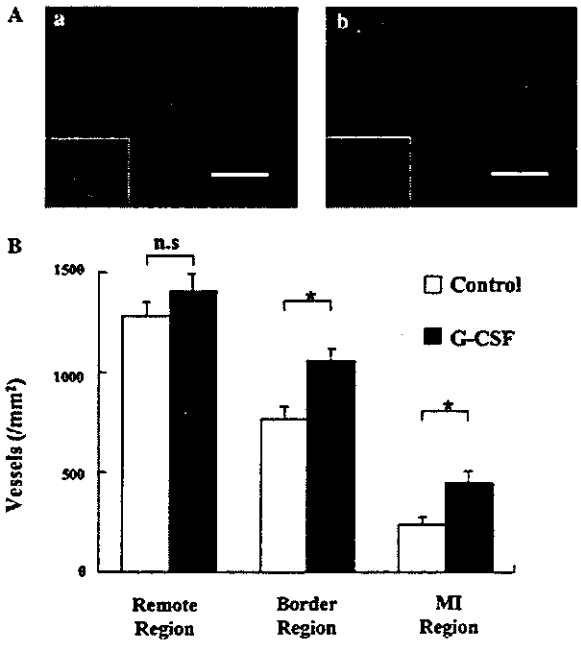

Fig. 2. Vessel analysis. (A) Endothelial cells of border zone myocardium were identified immunohistochemically using anti-von Willebrand factor (vWF) antibody (a, control group; b, G-CSF group), (magnification 100×, scale bar, 200 μm; magnification 400×, insets). (B) To measure the number of vessels, 15 fields were randomly chosen from remote, border, and MI regions in each sample ($n = 10$, each groups). Results are given as means ± SD ($n = 10$). *P <0.05.

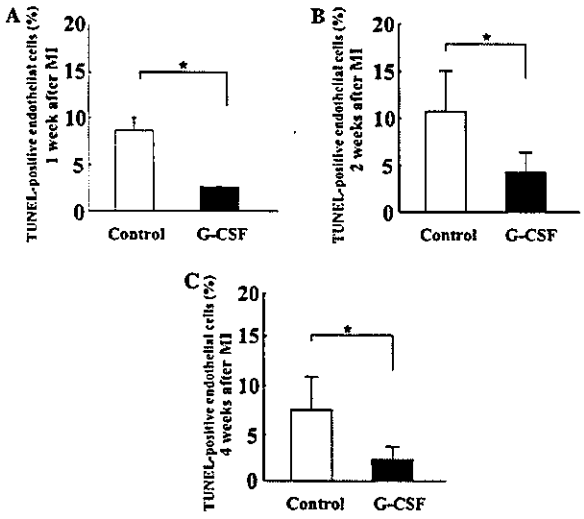

Fig. 3. Apoptotic cell death. The number of TUNEL-positive ECs was significantly smaller in the G-CSF treatment group than in control group at 1 week (A), 2 weeks (B), and 4 weeks (C), respectively. Results are given as means ± SD ($n = 10$). *P <0.05.

of apoptotic cells using TUNEL assay in the border region of MI heart. The number of TUNEL-positive cells in the border region was markedly smaller in the G-CSF treatment group (2 weeks, $3.3 \pm 1.5/10^3$ cells; 4 weeks, $5.6 \pm 2.1/10^3$ cells) than that in control group (2 weeks, $10.7 \pm 3.2/10^3$cells; 4 weeks, $12.6 \pm 4.7/10^3$cells). Very few apoptotic cardiomyocytes were recognized at all time points examined. Most of TUNEL-positive cells were infiltrated blood cells and a part of TUNEL-positive cells were vascular cells. To identify apoptotic cells, we performed double-staining using anti-vWF antibody and TUNEL. Almost all vascular cells positive for TUNEL expressed vWF, suggesting that apoptotic cells in the vessel are ECs. The number of TUNEL-positive ECs was significantly smaller in the G-CSF treatment group (1 week, $2.3 \pm 0.1\%$; 2 weeks, $4.2 \pm 1.9\%$; and 4 weeks, $2.6 \pm 2.1\%$) than in control group (1 week, $8.2 \pm 1.3\%$; 2 weeks, $11.0 \pm 4.4\%$; and 4 weeks, $8.1 \pm 3.9\%$) (Figs. 3A–C).

Akt and VEGF

Since Akt has been reported to play an important role in cell survival and angiogenesis [11], we next examined the activity of Akt. Western blot analysis demonstrated that the phosphorylated Akt1 was decreased markedly in the MI region and moderately in the border region (Figs. 4A and B). The G-CSF treatment increased the activity of Akt1 in all regions (Figs. 4A and B). VEGF is a member of angiogenic growth factor family and induces proliferation and survival of ECs [12]. The expression of VEGF protein was markedly

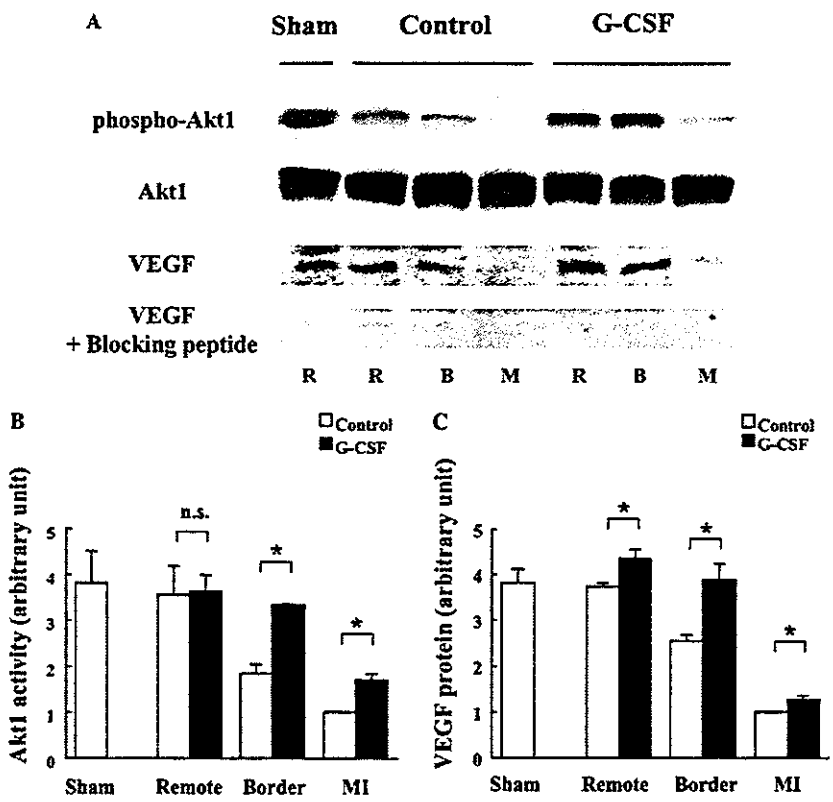

Fig. 4. Akt1 activity and VEGF protein level in myocardium. (A) Four weeks after MI, whole tissue lysates were extracted from hearts of three regions such as remote region, border region, and MI region, and subjected to Western blot analysis. The membranes were incubated with antibodies against Akt1, phospho-Akt1 or VEGF. VEGF blocking peptide was used to identify the band of VEGF. Results are representative of five independent experiments. R, remote region; B, border region; and M, MI region. (B,C) Quantitative analysis of phospho-Akt1 (B) and VEGF (C). Equal loading was validated by Ponceau S staining. Results are given as means ± SD ($n = 5$). *$P < 0.05$.

downregulated in the MI region (Figs. 4A and C). Downregulation of VEGF protein in the border region was milder in the G-CSF treatment group than in control group (Figs. 4A and C).

Discussion

In the present study, the G-CSF treatment prevented cardiac remodeling after MI in a preclinical swine model. The G-CSF treatment decreased apoptotic death of ECs and increased the number of vessels at the ischemic region, resulting in reduction in the infarcted size. G-CSF-induced activation of Akt and upregulation of VEGF may be associated with the beneficial effects.

Recently, BMSCs have been expected as the potential tool in regenerative medicine. Orlic et al. [2] have demonstrated that direct injection of BMSCs into the MI heart improves the cardiac function and mortality. Kamihata et al. [13] injected BM-derived mononuclear cells into the ischemic border and infarcted zone immediately after MI in pig, and demonstrated that myocardial blood flow was improved 3 weeks later. Moreover, Orlic et al. [6] examined whether treatment with cytokines increases mobilization of BMSCs to injured myocardium and promotes myocardial regeneration. After injection with rat stem cell factor (SCF) and recombinant human G-CSF once a day for 5 days, mice were subjected to ligation of left coronary artery. SCF and G-CSF were given for 3 more days. Cytokine-mediated mobilization of BM cells resulted in myocardial regeneration characterized by dividing cardiac myocytes and forming vascular structures 27 days after MI [6]. The treatment significantly improved cardiac function and reduced mortality. These results suggest that mobilized adult BMSCs transdifferentiate into cardiac myocytes, ECs, and VSMCs in ischemic myocardium and that cytokine therapy can be a noninvasive therapeutic strategy for regeneration of myocardium. However, their cytokine treatment was started before MI, and thus it is not clinically applicable. To elucidate whether the cytokine therapy can be clinically applied, we first examined whether subcutaneous injection of G-CSF, which is started from 24 h after

MI, has beneficial effects on cardiac function and cardiac remodeling in mice [8]. The G-CSF treatment started after MI was as effective as the pretreatment [8]. We next examined here as a preclinical study whether G-CSF treatment after MI prevents LV remodeling and improves cardiac function in large animals.

G-CSF has been reported to induce mobilization of BMSCs and EPCs as well as increase circulating WBC and granulocytes [14]. We first measured the numbers of WBC and granulocytes before and at 1, 3, 5, 7, and 28 days after MI in both G-CSF group and control group. The numbers of WBC and granulocytes were significantly increased in the G-CSF group. Although it remains unknown whether the increase in circulating WBC is associated with the prevention of LV remodeling after MI, BMSCs, and EPCs, whose mobilization could be induced by G-CSF, may be involved in cardiac regeneration and neovascularization [2,3,7,8,15].

The number of vessels in both ischemic and infarct regions was larger in the G-CSF treatment group than in control group. We have recently reported that the G-CSF treatment induces mobilization of BM cells into the infarct heart and that the BM cells are involved in an increase in vessel number [8]. In this study, we observed that the G-CSF treatment decreased the number of apoptotic ECs. On the other hand, we could not detect apoptotic cardiomyocytes in hearts at 2 days, 1 week, and 2 weeks after MI by double-staining with cTnT and TUNEL. Most of TUNEL-positive cells were infiltrated blood cells and a part of TUNEL-positive cells were observed at ECs. Although we could not demonstrate that G-CSF inhibits an increase in apoptotic cardiomyocytes after MI, our results suggest that G-CSF-induced increase in vessel number by a decrease in apoptotic vascular cells may prevent cardiomyocyte death after MI, resulting in the reduction of infarct size. It has been reported that G-CSF receptors exist in ECs and that G-CSF activates signal transduction pathways such as Jak/STAT and MAPK family in ECs [16,17]. Activation of Jak/STAT and ERK is known to induce survival through upregulating anti-apoptotic molecules including bcl-2 and bcl-xL. Although we have not examined whether G-CSF directly acts on ECs after MI, there is a possibility that G-CSF may directly prevent apoptosis of ECs by activating the survival signal pathways. To elucidate the mechanism of how the G-CSF treatment prevents LV remodeling after MI, we examined the expression of VEGF, a major member of angiogenic and survival growth factor family [12], in the myocardium after MI. The expression of VEGF in the ischemic region was more abundant in the G-CSF treatment group than in control group. G-CSF has been reported to activate a variety of intracellular signaling cascades such as Jak/STAT, Ras/Raf/MAP kinase, and Src family kinase pathways [14]. We have recently examined whether G-CSF acts directly on neonatal rat cardiomyocytes in vitro. Our results demonstrated that G-CSF induces an increase in expression levels of VEGF through Jak2/STAT3 pathway in cardiomyocytes (unpublished data). In nonproliferating terminally differentiated cells, G-CSF has been reported to activate the PI3K/Akt pathway [18]. Akt has been reported to play a critical role in cell survival and angiogenesis [11]. Furthermore, Mangi et al. [19] reported that Akt1 prevents remodeling and nearly normalizes cardiac performance. The G-CSF treatment increased the activity of Akt1 in the border region. Moreover, we recently found that G-CSF increases Akt1 activity in cardiac myocytes (unpublished data). Therefore, activation of Akt1 in the heart may indicate the activation of Akt1 in cardiomyocytes.

The patients with acute MI generally undergo percutaneous coronary intervention if the patients are hospitalized within the golden time. Therefore, the beneficial effects of G-CSF observed in the present study may be limited to the patients who do not undergo reperfusion. Further studies are needed to elucidate the cardioprotective effects of G-CSF on myocardial ischemia/reperfusion model.

Acknowledgments

The authors thank E. Fujita, R. Kobayashi, M. Watanabe, and Y. Ohtsuki for excellent technical assistance. This work was supported by a Grant-in-Aid for Scientific Research, Developmental Scientific Research, and Scientific Research on Priority Areas from the Ministry of Education, Science, Sports and Culture, and by the Program for Promotion of Fundamental Studies in Health Sciences of the Organization for Drug ADR Relief, R&D Promotion and Product Review of Japan (to I. Komuro).

References

[1] A.P. Beltrami, K. Urbanek, J. Kajstura, S.M. Yan, N. Finato, R. Bussani, B. Nadal-Ginard, F. Silvestri, A. Leri, C.A. Beltrami, P. Anversa, Evidence that human cardiac myocytes divide after myocardial infarction, N. Engl. J. Med. 344 (2001) 1750–1757.
[2] D. Orlic, J. Kajstura, S. Chimenti, I. Jakoniuk, S.M. Anderson, B. Li, J. Pickel, R. McKay, B. Nadal-Ginard, D.M. Bodine, A. Leri, P. Anversa, Bone marrow cells regenerate infarcted myocardium, Nature 410 (2001) 701–705.
[3] K.A. Jackson, S.M. Majka, H. Wang, J. Pocius, C.J. Hartley, M.W. Majesky, M.L. Entman, L.H. Michael, K.K. Hirschi, M.A. Goodell, Regeneration of ischemic cardiac muscle and vascular endothelium by adult stem cells, J. Clin. Invest. 107 (2001) 1395–1402.
[4] L.B. To, D.N. Haylock, P.J. Simmons, C.A. Juttner, The biology and clinical uses of blood stem cells, Blood 89 (1997) 2233–2258.
[5] D.C. Link, Mechanisms of granulocyte colony-stimulating factor-induced hematopoietic progenitor-cell mobilization, Semin. Hematol. 37 (2000) 25–32.

[6] D. Orlic, J. Kajstura, S. Chimenti, F. Limana, I. Jakoniuk, F. Quaini, B. Nadal-Ginard, D.M. Bodine, A. Leri, P. Anversa, Mobilized bone marrow cells repair the infarcted heart, improving function and survival, Proc. Natl. Acad. Sci. USA 98 (2001) 10344–10349.

[7] A.A. Kocher, M.D. Schuster, M.J. Szabolcs, S. Takuma, D. Burkhoff, J. Wang, S. Homma, N.M. Edwards, S. Itescu, Neovascularization of ischemic myocardium by human bone-marrow-derived angioblasts prevents cardiomyocyte apoptosis, reduces remodeling and improves cardiac function, Nat. Med. 7 (2001) 430–436.

[8] M. Ohtsuka, H. Takano, Y. Zou, H. Toko, H. Akazawa, Y. Qin, M. Suzuki, H. Hasegawa, H. Nakaya, I. Komuro, Cytokine therapy prevents left ventricular remodeling and dysfunction after myocardial infarction through neovascularization, FASEB J. 18 (2004) 851–853.

[9] T. Asahara, H. Masuda, T. Takahashi, C. Kalka, C. Pastore, M. Silver, M. Kearne, M. Magner, J.M. Isner, Bone marrow origin of endothelial progenitor cells responsible for postnatal vasculogenesis in physiological and pathological neovascularization, Circ. Res. 85 (1999) 221–228.

[10] A. Abbate, G.G.L. Biondi-Zoccai, A. Baldi, Pathophysiologic role of myocardial apoptosis in post-infarction left ventricular remodeling, J. Cell. Physiol. 193 (2002) 1243–1250.

[11] I. Shiojima, K. Walsh, Role of Akt signaling in vascular homeostasis and angiogenesis, Circ. Res. 90 (2002) 1243–1250.

[12] N. Ferrara, Role of vascular endothelial growth factor in regulation of physiological angiogenesis, Am. J. Physiol. Cell Physiol. 280 (2001) C1358–C1366.

[13] H. Kamihata, H. Matsubara, T. Nishiue, S. Fujiyama, Y. Tsutsumi, R. Ozono, H. Masaki, Y. Mori, O. Iba, E. Tateishi, A. Kosaki, S. Shintani, T. Murohara, T. Imaizumi, T. Iwasaka, Implantation of bone marrow mononuclear cells into ischemic myocardium enhances collateral perfusion and regional function via side supply of angioblasts, angiogenic ligands, and cytokines, Circulation 104 (2001) 1046–1052.

[14] B.R. Avalos, Molecular analysis of the granulocyte colony-stimulating factor receptor, Blood 88 (1996) 761–777.

[15] T. Takahashi, C. Kalka, H. Masuda, D. Chen, M. Silver, M. Kearney, M. Magner, J.M. Isner, T. Asahara, Ischemia- and cytokine-induced mobilization of bone marrow-derived endothelial progenitor cells for neovascularization, Nat. Med. 5 (1999) 434–438.

[16] E. Bocchietto, A. Guglielmetti, F. Silvagno, G. Taraboletti, G.P. Pescarmona, A. Mantovani, F. Bussolino, Proliferative and migratory responses of murine microvascular endothelial cells to granulocyte colony-stimulating factor, J. Cell. Physiol. 155 (1993) 89–95.

[17] B. Fuste, R. Mazzara, G. Escolar, A. Merino, A. Ordinas, M. Diaz-Ricart, Granulocyte colony-stimulating factor increases expression of adhesion receptors on endothelial cells through activation of p38 MAPK, Haematologica 89 (2004) 578–585.

[18] F. Dong, A.C. Larner, Activation of Akt kinase by granulocyte colony-stimulating factor (G-CSF): evidence for the role of a tyrosine kinase activity distinct from the janus kinases, Blood 95 (2000) 1656–1662.

[19] A.A. Mangi, N. Noiseux, D. Kong, H. He, M. Rezvani, J.S. Ingwall, V.J. Dzau, Mesenchymal stem cells modified with Akt prevent remodeling and restore performance of infarcted hearts, Nat. Med. 9 (2003) 1195–1201.

Available online at www.sciencedirect.com
SCIENCE DIRECT
Journal of Molecular and Cellular Cardiology 36 (2004) 175–183
Journal of Molecular and Cellular Cardiology
www.elsevier.com/locate/yjmcc

Review Article

Vascular cell senescence and vascular aging☆

Tohru Minamino, Hideyuki Miyauchi, Toshihiko Yoshida, Kaoru Tateno, Takeshige Kunieda, Issei Komuro *

Department of Cardiovascular Science and Medicine, Chiba University Graduate School of Medicine, 1-8-1 Inohana, Chuo-ku, Chiba 260-8670, Japan

Received 20 August 2003; received in revised form 15 November 2003; accepted 17 November 2003

Abstract

Vascular cells have a finite lifespan when cultured in vitro and eventually enter an irreversible growth arrest called "cellular senescence". A number of genetic animal models carrying targeted disruption of the genes that confer the protection against senescence in vitro have been reported to exhibit the phenotypes of premature aging. Similar mutations have been found in the patients with premature aging syndromes. Many of the changes in senescent vascular cell behavior are consistent with the changes seen in age-related vascular diseases. We have demonstrated the presence of senescent vascular cells in human atherosclerotic lesions but not in non-atherosclerotic lesions. Moreover, these cells express increased levels of pro-inflammatory molecules and decreased levels of endothelial nitric oxide synthase, suggesting that cellular senescence in vivo contributes to the pathogenesis of human atherosclerosis. One widely discussed hypothesis of senescence is the telomere hypothesis. An increasing body of evidence has established the critical role of the telomere in vascular cell senescence. Another line of evidence suggests that telomere-independent mechanisms are also involved in vascular cell senescence. Activation of Ras, an important signaling molecule involved in atherogenic stimuli, induces vascular cell senescence and thereby promotes vascular inflammation in vitro and in vivo. It is possible that mitogenic-signaling pathways induce telomere-dependent and telomere-independent senescence, which results in vascular dysfunction. Further understanding of the mechanism underlying cellular senescence will provide insights into the potential of antisenescence therapy for vascular aging.

Keywords: Senescence; Aging; Atherosclerosis; Telomere; Ras; Akt; Inflammation; Cyclin-dependent kinase inhibitor

1. Introduction

Cellular senescence is the limited ability of primary human cells to divide when cultured in vitro and is accompanied by a specific set of phenotypic changes in morphology, gene expression and function. These changes in phenotype have been implicated in human aging [1]. This hypothesis, the hypothesis of cellular aging, was first described by Hayflick [2] and supported by evidence that cellular senescence and the division potential of human primary cultures are dependent on donor age [3] and that the growth potential of cultures correlates well with mean maximum lifespan of the species from which the cultures are derived [4]. Human primary cultures derived from the patients with premature aging syndromes, such as Werner syndrome and Bloom syndrome, are known to have shorter lifespan than the cultures from age-matched healthy populations [5], thus supporting the hypothesis of aging. However, until recently, little attention has been paid on the potential impact of vascular cell senescence in vivo on age-related vascular disorders.

In the past decades, significant progress has been made in our understanding of the mechanisms underlying cellular senescence. One widely discussed hypothesis is the telomere hypothesis of senescence [6]. A growing body of evidence has demonstrated a critical role of telomere and telomerase in regulating not only cellular lifespan but also organismal aging. However, recent findings suggest that cellular senescence can also be induced by DNA damage, cellular stress or oncogenic activation, which is independent of replicative age [7]. For example, the constitutive activation of mitogenic stimuli by expression of oncogenic Ras induces senescent phenotypes [8–10]. Thus, it is possible that atherogenic stimuli increase cell turnover at the sites of atherosclerosis, thereby promoting telomere shortening, whereas it also re-

☆ The review process for this manuscript was handled by Consulting Editor, Eduardo Marban.

* Corresponding author. Tel.: +81-43-226-2097; fax: +81-43-226-2557
E-mail address: komuro-tky@umin.ac.jp (I. Komuro).

doi:10.1016/j.yjmcc.2003.11.010

sults in activation of proliferative signals that potentially induce senescence independent of telomere shortening.

In this review, we will describe recently accumulating evidence that supports the hypothesis of cellular aging in the vasculature and discuss the potential of antisenescence therapy for age-related human vascular disorders.

2. Occurrence of vascular cell senescence in vivo

Vascular cells have a finite lifespan in vitro and eventually enter an irreversible growth arrest called cellular senescence. Flattened and enlarged cell morphology is known to be one of the characteristics of cellular senescence [11]. Expression of negative regulators for the cell cycle machinery, such as p53 and p16, is increased with cell division and thereby promotes growth arrest [12]. Primary cultured cells undergoing cellular senescence in vitro express the increased activity of β-galactosidase (β-gal) when assayed at pH 6, which is distinguishable from endogenous lysosomal β-gal activity that can be detected at pH 4. This activity, senescence-associated β-gal (SA β-gal) activity, has been shown to correlate with cellular aging and thus is regarded as a biomarker for cellular senescence [13]. The in vitro growth properties of vascular cells derived from human atherosclerotic plaque are impaired, and they develop senescence earlier than those from normal lesions [14,15]. The histology of the lesions of human atherosclerosis has been extensively studied, and these studies have demonstrated that there are endothelial cells (ECs) and vascular smooth muscle cells (VSMCs) that exhibit the morphological features of cellular senescence [16,17]. These suggest the occurrence of cellular senescence in vivo. Recently, this notion has been confirmed by cytochemical analysis in vivo using SA β-gal activity. Fenton et al. [18] have successfully detected SA β-gal-positive vascular cells in rabbit carotid arteries subjected to vascular injury. With repeated denudation, the accumulation of SA β-gal-positive cells was markedly enhanced. The authors have recently demonstrated SA β-gal-positive vascular cells in human atherosclerotic plaque of the coronary arteries obtained from the patients who had ischemic heart disease [19]. SA β-gal-positive cells were predominately localized on the luminal surface of atherosclerotic plaque and identified as ECs, but no positive cells were observed in the internal mammary arteries from the same patients where atherosclerotic changes were minimally observed. In advanced plaque, however, SA β-gal-positive VSMCs were detected in the intima but not in the media [20], which may represent extensive replication in the lesions, as observed in the arteries subjected to double-denudation (Fig. 1). SA β-gal-positive cells exhibit increased expression of p53 and p16, alternative markers for cellular senescence, in human atheroma, suggesting the further evidence of in vivo senescence. These cells also show impaired function, such as the decreased expression of endothelial nitric oxide synthase (eNOS) and the increased expression of pro-inflammatory molecules

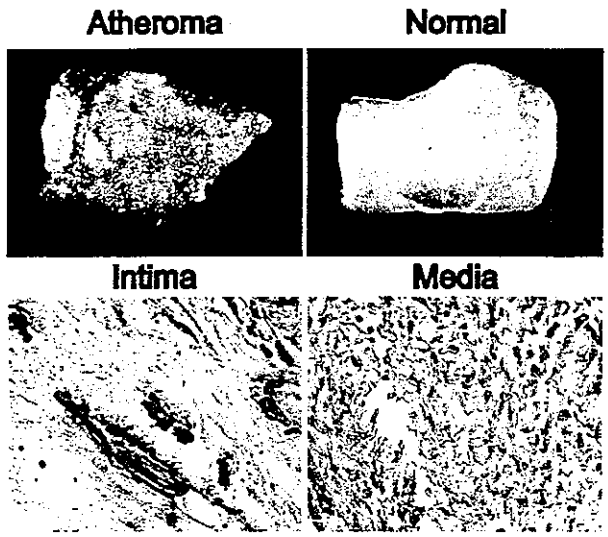

Fig. 1. Senescent vascular cells in human atheroma. Photographs of the luminal surface of human atheroma (atheroma, left) and non-atherosclerotic normal artery (normal, right) stained with SA β-gal staining. SA β-gal activity was observed in human atheroma but not in normal arteries (upper panel). A double staining for SA β-gal and α-smooth muscle actin of the sections of atheroma identified SA β-gal-positive cells as VSMCs in the intima but not in the media (lower panel).

[20]. Thus, cellular senescence in vivo may contribute to the pathogenesis of vascular aging.

3. Role of cellular senescence in vascular pathophysiology

Age-associated changes in the blood vessels include a decrease in compliance and an increase in inflammatory response that promote atherogenesis [21]. It has also been reported that angiogenesis is impaired with advanced age [22,23], whereas aging decreases the antithrombogenic property of the endothelium [24]. A number of studies have reported that many of the changes in senescent vascular cell behavior are consistent with known changes seen in age-related vascular diseases, suggesting a critical role of cellular senescence in vascular pathophysiology. The production of nitric oxide (NO) and the eNOS activity are reduced in senescent human ECs [25]. Induction of NO production by shear stress is also decreased in senescent ECs [26]. A decline in the eNOS activity of senescent ECs is attributable to a decrease in expression of eNOS protein as well as in eNOS phosphorylation mediated by Akt [27]. The levels of prostacyclin production are significantly decreased with in vitro aging of ECs [28], whereas senescent ECs upregulate plasminogen activator inhibitor-1 [29]. All these alterations are likely involved in the impairment of endothelium-dependent vasodilation but also increased sensitivity of thrombogenesis in human atherosclerosis. The interaction between monocytes and ECs is enhanced by EC senescence [30], thereby promoting atherogenesis. This appears to be mediated by upregulation of adhesion molecules and pro-inflammatory

cytokines as well as a decrease in the production of NO in senescent ECs [19,26]. It is reported that the ability to form capillary structures in vitro is reduced in senescent ECs [31]. Bone marrow-derived circulating endothelial progenitor cells (EPCs) are known to participate in postnatal neovascularization and vascular repair [32,33]. The in vitro growth property and function of bone marrow-derived EPCs are impaired in the patients with coronary artery disease and negatively correlate with risk factors including age [34,35]. Thus, aging may promote senescence of EPCs as well as ECs, resulting in decreases in angiogenesis and vascular healing.

4. Telomere-dependent vascular cell senescence

Telomeres are non-nucleosomal DNA–protein complexes at the end of chromosomes that serve as protective caps and are substrates for specialized replication mechanisms. As a consequence of semi-conservative DNA replication, the extreme termini of chromosomes are not duplicated completely, resulting in successive shortening of telomeres with each cell division. Critically short telomere was thought to trigger the onset of cellular senescence, but recent studies suggest that the single-strand telomeric overhang and associated proteins are key components for signals of senescence [36,37]. Telomerase is a ribonucleoprotein that adds telomeres onto chromosome ends with its RNA moiety as a template. Forced expression of the catalytic component of telomerase TERT in telomerase-negative human fibroblasts results in the stabilization of telomere length and extension of cell lifespan [38]. This observation has established the importance of telomere shortening in human cellular senescence. It has been also reported that there is another mechanism of telomere maintenance without telomerase activity, called telomerase-independent alternative lengthening of telomeres (ALT) [39]. In the field of vascular biology, it has been shown that telomere shortening with cell divisions occurs in human-cultured ECs and VSMCs, and that introduction of TERT extends cell lifespan of human ECs and VSMCs, suggesting a critical role of telomere shortening in vascular cell senescence as well [31,40,41]. It is likely that shortened telomeres are in some way sensed in a cell, and that a pathway is activated that results in exit from cell cycle (Fig. 2). The p53, p21 and p16 proteins and their downstream effectors are important for cellular senescence, and thus are likely to be a part of the telomere-response pathway. However, less is known about what links telomeres and these factors. Until present, several telomeric-binding proteins have been identified that contribute to the integrity of telomere functions and are potentially involved in the telomere-response pathway [42]. These include protection of telomeres-1 (Pot-1) [43], Ku [44], telomeric repeat-binding factor 1 and 2 (TRF1 and TRF2, respectively) [45]. Pot-1 is identified as a telomeric protein that binds to a tip of telomere and is thought to constitute the telomere shortening signal [46]. The protein

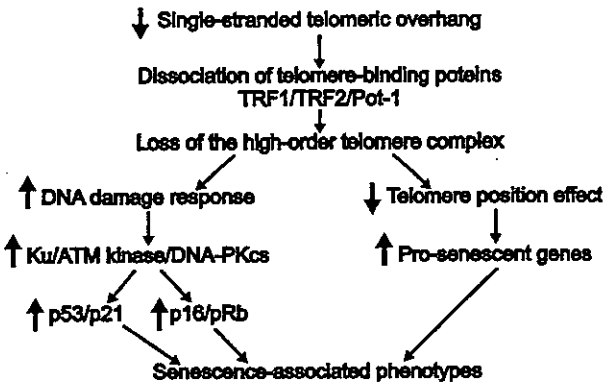

Fig. 2. Putative telomere-responsible pathways. As cells age, single-stranded telomeric overhangs are eroded, resulting in the dissociation of telomeric proteins. Loss of the high-order telomere complex is recognized as DNA breaks, thereby activating the molecules involving DNA repair that also play a critical role for telomere maintenance. These signals of DNA damage response are conducted to the cell cycle machinery. Telomere dysfunction also results in a release of telomere position effects that have the impact on expression of the genes at subtelomeric regions.

Ku, originally defined by its role in the repair of chromosomal DNA breaks, is found at telomeres and is necessary for normal telomere maintenance and functions. Genetic ablation studies demonstrated an essential role of Ku in mediating the telomere-response pathway [47]. Likewise, the catalytic subunit of the DNA-dependent protein kinase complex [48] and ATM kinase [49], both of which function in the double-strand break repair, have been implicated in the signal pathway of telomere shortening. Recently, it has been proposed that telomeres form large duplex loops, and telomeric proteins, TRF1 and TRF2, are essential for their formation [50,51]. Particularly, inhibition of TRF2 function is reported to cause cellular senescence in a p53/p16-dependent manner [19,52]. Thus, it is supposed that, as a result of telomere shortening, the efficacy of forming a high-order telomeric complex is impaired, leading to a release of various telomeric proteins from telomeres that elicit signals for cellular senescence (Fig. 2). Cytologically, telomeric regions are heterochromatic, implying that local DNA folding is increased. Positioning a gene in a telomeric heterochromatic region can impose telomere position effect on that gene. Telomere position effect, which has been characterized in the yeast and recently in human cells, is known to induce the reversible silencing of the gene [53]. Consequently, the modification of gene expression by telomere position effect may also contribute to the signaling pathway for cellular senescence.

5. Telomere shortening and vascular dysfunction

There is evidence indicating that telomere shortening occurs in human vasculature, which may be related to age-associated vascular diseases [54]. In most of the previous reports mentioned, changes in cell phenotypes associated with senescence were studied in vascular cell populations

undergoing replicative senescence, thus suggesting telomere-dependent vascular dysfunction. However, it remains unclear whether phenotypic changes in senescent vascular cells result from telomere dysfunction. Inhibition of TRF2 has been shown to induce either cellular senescence or apoptosis in various cells by destroying telomere loop structure [51,55]. The authors have demonstrated that the introduction of a dominant-negative form of TRF2 into human ECs induces a growth arrest with phenotypic characteristics of cellular senescence [19]. Telomere dysfunction significantly increases expression of pro-inflammatory molecules and reduces the activity of eNOS, suggesting a causal link between telomere and vascular dysfunction associated with senescence.

Telomerase-deficient mice have been developed and found to reveal a normal phenotype at the first generation presumably because of mice having much longer telomeres [56,57]. Telomeres are shortened with successive generations, and they become infertile at the sixth generation due to the impairment of reproductive system. Some aspects of the late generation mice mimic age-associated phenotypes. They exhibit shortened lifespan and a reduced capacity to respond to stress, such as wound healing and hematopoietic ablation [58]. The ability of neovascularization is reduced in the late generation of telomerase-deficient mice [59]. Decreased vessel formation may be attributable to the impaired function and replicative capacity of ECs induced by telomere shortening. Recently, the heart in late generation of telomerase-deficient mice has been shown to mimic the end-stage-dilated cardiac myopathy in humans [60].

6. Telomerase

Since early studies reported that telomerase activity was detected in cancer cells but not normal somatic cells, the idea emerged that telomerase activity might be essential for tumor growth [61]. Multiple tumor-suppressor pathways are likely to repress telomerase expression in normal somatic cells [62]. Increasing evidence has suggested that telomerase activity regulates cell proliferation in normal somatic cells by telomere lengthening or upregulating growth-controlling genes in a telomere length-independent manner [57,63]. Human ECs and VSMCs express telomerase activity, which is drastically activated by mitogenic stimuli via a protein kinase C-dependent pathway [64] but the activity declined with in vitro aging due to a decrease in expression of TERT, leading to telomere shortening and cellular senescence [41,65]. Introduction of TERT prevents endothelial dysfunction associated with senescence, such as a decrease in eNOS activity and an increase in monocyte binding to ECs [19,26]. Immortalized human ECs (TERT-ECs) have been established by introduction of TERT [31]. TERT-ECs appear to retain EC characteristics including various cell surface markers. When examined in Matrigel, they form capillary-like structures in response to extracellular matrix signals as efficiently as early passage of ECs, whereas senescent or transformed ECs do not. In addition, TERT-ECs are more resistant to apoptotic induction than pre-senescent ECs. They maintain a normal growth control and exhibit no transformed phenotype. These telomerized human ECs are functional in vivo as demonstrated by the Matrigel implantation mouse model [66]. In this model, whereas primary human EC-derived vessel density decreased with time after implantation, telomerized ECs maintained durable vessels, indicating that telomerase activity is important for the maintenance of a microvascular phenotype.

7. Telomere-independent vascular cell senescence

Signals other than extended proliferation have been shown to result in cells developing a phenotype indistinguishable from that of senescent cells at the end of their replicative lifespan. For example, the constitutive activation of mitogenic stimuli by expression of oncogenic Ras or E2F induce a senescent phenotype [8,67]. Cellular senescence triggered by mitogenic stimuli is independent of replicative age, and these signals act before the replicative limits of cells. Hence, it is apparently telomere independent and thus termed as premature senescence. The constitutive activation of Ras provokes premature senescence in vascular cells, which is associated with accumulation of the proteins p53 as well as p16 [20]. Activation of extracellular signal-regulated kinase (ERK) appears to be critical for Ras-induced senescence since inhibition of ERK restores cell growth arrest elicited by Ras activation [20], whereas introduction of an active form of ERK results in premature senescence involving p53 and p16 [9]. p38 mitogen-activated protein kinase (MAPK) is also implicated in Ras-induced senescence. p38 MAPK is activated in a ERK-dependent fashion, thus indicating that Ras promotes premature senescence by sequentially activating the ERK and p38 MAPK pathway [68].

8. Cell cycle regulators

It is clear that cellular senescence entails the activation of several tumor-suppressor proteins and inactivation of several oncoproteins, each of which ultimately engages either the p53 or pRb pathway and interacts with each other at multiple levels (Fig. 3). p53 activity and in some cases protein levels are increased in senescent cells. The mechanisms responsible for p53 activation in senescent cells remain elusive, however some molecular details are emerging. One cause of p53 activation may be an increase in expression of p14, a tumor-suppressor protein encoded by the INK4a locus. p14 activates p53 through a mechanism involving sequestration of MDM2, a protein that promotes degradation of p53 [69]. p14 is induced by oncogenic Ras and E2F [70], whereas TBX2, a member of T-box family of transcription factors, suppresses p14 expression [71]. Another cause of p53 activation is the